Hamiltonian truncation in one-dimensional long-range CFTs

Leonardo S. Cardinale*

Laboratoire de Physique de l'Ecole Normale Supérieure – PSL, Paris, France $M2\ Intern$

Miguel F. Paulos[†]

Laboratoire de Physique de l'Ecole Normale Supérieure – PSL, Paris, France Supervisor

June 2025

We motivate the study of Hamiltonian truncation through two simple examples, namely the one-dimensional long-range Ising and Lee-Yang models, which are closely related to ϕ^4 and ϕ^3 theory respectively. These are some of the simplest non-trivial conformal field theories which can be defined in one dimension. We start by motivating these CFTs physically, discussing on the one hand how they emerge as Landau-Ginzburg theories for Ising spins on the lattice, and on the other how they can naturally be viewed as the dimensional reduction of a massive local free field in anti-de Sitter space with boundary interactions. The latter approach is particularly enlightening, since our theory can then be viewed as living on ∂AdS_2 , which is conformal to the one-dimensional cylinder $\mathbb{R} \times S^0$. As such, a quantum field-theoretic problem is converted into a two-site quantum mechanical one with a discrete spectrum, which thus lends itself particularly well to Hamiltonian truncation. Upon introducing the general idea of Hamiltonian truncation, we subsequently build the relevant Hamiltonian in radial quantization, and then solve for its spectrum numerically. In order to study the theory at its conformal fixed point, we impose constraints on the spectrum, namely the existence of a vacuum state of vanishing energy, the existence of a primary operator of dimension Δ_{ϕ} , a descendant of dimension $\Delta_{\phi}+1$ and the equation of motion. Concretely, this requires introducing a cosmological constant, as well as monomial counter-terms to the bare Hamiltonian. The spectra computed in this manner agree with perturbative results derived using an ε -expansion. Lastly, we discuss ways of improving Hamiltonian truncation at fixed UV cutoff by introducing effective interactions which account for higher energy states which have been integrated out.

Contents

1	\mathbf{Intr}	roduction and summary	2
	1.1	Introduction	2
	1.2		
2	Con	nstruction of LORI and LORALY	4
	2.1	Landau-Ginzburg approach	4
	2.2	Construction of long-range theories on the boundary of AdS spacetime	6
	2.3	Theories on the cylinder	7
3	Ren	normalization group analysis	7
	3.1	Preliminary remarks and a comment regarding non-locality	7
	3.2		8
		3.2.1 Two-loop renormalization of the vertex	9
		3.2.2 Fixed point and anomalous dimension of ϕ^4 to two-loop order	10
		3.2.3 Anomalous dimension of ϕ^2 to two-loop order	
		3.2.4 Anomalous dimension of ϕ^n to one-loop order	
	3.3	· · · · · · · · · · · · · · · · · · ·	
	0.0	3.3.1 Two-loop renormalization of the vertex	
		3.3.2 Fixed point and anomalous dimension of ϕ^3 to two-loop order	

^{*}leonardo.cardinale@phys.ens.fr

[†]miguel.paulos@phys.ens.fr

4	Hamiltonian truncation	13
	4.1 Setup	
	4.2 Radial quantization and the state-operator correspondence	14
	4.3 Radial quantization of the generalized free field	
	4.4 Tuning to LORI and LORALY	16
	4.5 Comparison with Rayleigh-Schrödinger perturbation theory	17
	4.6 Numerical workflow and results	18
5	Effective Hamiltonians and renormalization	20
	5.1 Next-to-leading order effective Hamiltonian	20
	5.2 Numerical results	24
	5.3 UV divergences	25
	5.4 Renormalization of the effective theory: the general picture	
	5.5 Renormalization of one-dimensional effective theories	
6	Conclusion	31
\mathbf{A}	Useful integrals	31
	A.1 GFF propagator	31
	A.2 Convolution formula	
	A.3 Extraction of divergences	
В	Diagrammatics	33
	B.1 Hard diagram in the renormalization of ϕ^2	33
	B.2 Anomalous dimension of ϕ^4 to one-loop order	
\mathbf{C}	Anomalous dimensions from β -functions	34

1 Introduction and summary

1.1 Introduction

Quantum field theory is at the crux of many fundamental problems in theoretical physics, from particle physics to condensed matter physics. While QFT in the weak coupling limit is well-understood, the strong coupling limit remains elusive, and is at the heart of understanding inherently non-perturbative phenomena such as confinement in QCD. In order to develop an understanding of QFT beyond perturbation theory, one promising approach is the bootstrap program. This program amounts to leveraging general principles, such as symmetry and unitarity, to derive the dynamics of a given theory. This works particularly well for conformal field theories [1], where additional spacetime symmetries significantly constrain correlation functions.

While conformal symmetry isn't realized for most QFTs, particularly those describing fundamental interactions, the study of CFT can be strongly motivated by the two following points. On the one hand, CFTs are often endpoints of renormalization group flows, and hence they provide natural points in theory space to study. Furthermore, characterizing these fixed points allows one to constrain the dynamics of the potentially more realistic QFTs belonging to the corresponding universality class. On the other hand, the AdS/CFT correspondence [2] tells us that the study of a QFT in AdS_{d+1} is intimately related to that of a CFT on the d-dimensional boundary ∂AdS_{d+1} . Since the bulk theory doesn't have to be conformally invariant a priori, this suggests that deriving the CFT data from the boundary theory can help characterize the dynamics of a vast array of QFTs. More strikingly, these theories also include gravity, and hence CFTs can be viewed as encoding quantum gravity.

Since CFTs are more tractable than QFTs, but nevertheless encode dynamics of more general QFTs as described above, a first but crucial first step to tackling strongly coupled QFT is the study of strongly coupled CFT. A popular approach is the conformal bootstrap. Indeed, a CFT is fully characterized by a set of operators and their two and three-point data, such that crossing symmetry is obeyed by all sets of four operators in the theory. Given four operators $\mathcal{O}_1(x_1)$, $\mathcal{O}_2(x_2)$, $\mathcal{O}_3(x_3)$, $\mathcal{O}_4(x_4)$, associativity of the OPE leads to the so-called crossing equation

$$\sum_{\mathcal{O}} \lambda_{12\mathcal{O}} \lambda_{34\mathcal{O}} G_{\Delta_{\mathcal{O}}}(u, v) = \sum_{\mathcal{O}} \lambda_{13\mathcal{O}} \lambda_{24\mathcal{O}} G_{\Delta_{\mathcal{O}}}(u, v) , \qquad (1.1)$$

where the λ factors are three-point data, $\Delta_{\mathcal{O}}$ is a scaling dimension, u, v are conformally invariant cross-ratios formed using x_1, x_2, x_3, x_4 and the $G_{\Delta_{\mathcal{O}}}$'s are some functions known as conformal blocks. Imposing this equation to all sets

of operators $\{\mathcal{O}_1, \mathcal{O}_2, \mathcal{O}_3, \mathcal{O}_4\}$ would in principle, combined with symmetries which characterize a given theory or assumptions regarding unitarity, and more recently locality [3, 4], fully characterize a given theory, and solving all crossing equations would lead to the complete corresponding set of CFT data $\{\lambda_{ijk}, \Delta_l\}$. However, this is unfeasible in practice, and one merely imposes crossing symmetry to a finite subset of operators. This can be done analytically, particularly in two dimensions [5], but mainly numerically in higher dimensions [1, 6]. This leads to numerical bounds on CFT data, which can nevertheless be rendered very precise [7].

There are usually more tools for studying low-dimensional – typically 1D, 2D or (1+1)D – theories, and more results be they analytic or numeric. In one dimension, extensive work has been conducted on the bootstrap side [8–11], which leverages so-called analytic extremal functionals to study solutions of bootstrap equations. Other methods complementary to the bootstrap have also been suggested, such as those involving tensor network states, be it for statistical mechanical models [12–16] or relativistic field theory [17–21]. These methods accompany an already well-established toolbox, such as lattice gauge theory – which is particularly studied in the context of quantum chromodynamics [22] – as well as the density matrix renormalization group (DMRG), standard in the condensed matter community [23, 24].

In this work, we address an avenue which, until recently, hasn't been extensively explored, namely Hamiltonian truncation. Hamiltonian truncation generally involves the study of a Hamiltonian written as the sum of a solvable part H_0 , and an interaction term V. The method is straightforward in principle: simply project the Hamiltonian of a given theory onto a lower-dimensional Hilbert space, and diagonalize it. This subspace \mathcal{H}_{eff} of the ambient Hilbert space \mathcal{H} is typically chosen by using an energy – or scaling dimension in radial quantization – cutoff Δ_T such that elements of the eigenbasis of \mathcal{H} associated to the Hamiltonian H are thrown away unless their energy is less than Δ_T . One then hopes that the restriction of H to \mathcal{H}_{eff} , accurately predicts the low-energy spectrum of the theory:

$$\forall |i\rangle, |f\rangle \in \mathcal{H}_{\text{eff}}, \langle i|H_{\text{eff}}|f\rangle \approx \langle i|H|f\rangle.$$
 (1.2)

While this idea seems natural in standard quantum mechanics, it was apparently first used for QFT in [25]. Hamiltonian truncation was subsequently applied to the study of two-dimensional conformal field theories, where it was referred to as the 'truncated conformal space approach' (TCSA) [26, 27]. Subsequent applications of this method were reviewed in [28]. More recently, there has been a revived interest in Hamiltonian truncation for QFT and CFT, where it has been met with some success particularly in two-dimensional models [29–48].

Since the dimension of spacetime becomes a significant constraint, we start with the simplest non-trivial case, namely that of a one-dimensional CFT. Two-dimensional CFT is also largely within reach in Hamiltonian truncation, in fact one has access to a plethora of solvable theories, for example minimal models [49], which can play the role of H_0 . In other dimensions, we generally start from a generalized free field theory however, and we'll be doing so in our study of one-dimensional CFTs. Such CFTs can be IR-regulated on the cylinder, or similarly considered as living on the one-dimensional cylindrical boundary of AdS_2 , which is essentially given by two parallel lines whose coordinates can be viewed as time. We therefore gain access to the tools of 'ordinary' quantum mechanics, and 'well-behaved' Hamiltonians with discrete spectra which are in principle very sparse.

Our study focuses on non-local theories, known as the long-range Ising model (LORI), and the long-range Lee-Yang model (LORALY), which are intimately related to ϕ^4 and ϕ^3 theories in AdS₂. These are the simplest non-trivial examples of a family of interacting long-range theories with ϕ^n interactions. Incidentally, one might wonder why we don't address the even simpler case of a local theory in one dimension, before moving on to non-local ones. This is mainly due to the fact that local CFTs in one dimension are necessarily topological, i.e. observables in such theories do not depend on distances between insertions. Indeed, the stress tensor T in a CFT is traceless, but since it only has a single component it vanishes. Yet T coincides with the generator of 'spacetime' translations in d = 1, which implies that a local operator $\mathcal{O}(x)$ is shifted by a term proportional to $\delta\mathcal{O}(x) = [T, \mathcal{O}(x)] = 0$ under an infinitesimal translation. This statement subsequently lifts to correlation functions of local operators, which are hence position-independent. In order to recover non-trivial behavior, we must work with conformally invariant theories devoid of a stress tensor, which leads to introducing non-local generalized free fields.

1.2 Summary

The models we study in this work – the long-range Ising and Lee-Yang models – are respectively associated to the following actions in one dimension:

$$S[\phi] = \frac{\mathcal{K}_{\sigma}}{2} \int dx dy \frac{\phi(x)\phi(y)}{|x - y|^{1+\sigma}} + \frac{\lambda}{4!} \int dx \phi^4(x), \qquad (1.3)$$

$$S[\phi] = \frac{\mathcal{K}_{\sigma}}{2} \int dx dy \frac{\phi(x)\phi(y)}{|x - y|^{1+\sigma}} + \frac{ig}{3!} \int dx \phi^3(x).$$
 (1.4)

where $\sigma=1-2\Delta_{\phi}$ for a scaling dimension Δ_{ϕ} , and \mathcal{K}_{σ} is some σ -dependent normalization. Note that (1.3) is a unitary theory, the action being Hermitian, while (1.4) is not. The former is nothing but the Landau-Ginzburg theory corresponding to the long-range Ising model defined on the lattice at its critical temperature. The latter is less straightforward. It is still a a Landau-Ginzburg action, associated to a long-range Ising model in a constant magnetic field h, except we now take h close to a zero of the corresponding partition function. These points are discussed in more detail in section 2.1. Alternatively, these models can also be constructed on the boundary of AdS_2 – as discussed in section 2.2 – starting from the theory of a free massive scalar field $\Phi(z,x)$ in the bulk with boundary interactions, and integrating out the bulk degrees of freedom to arrive at the theory governing $\phi(x) = \Phi(0,x)$, which is nothing but (1.3) or (1.4). These QFTs flow to non-trivial fixed points if we respectively take $\Delta_{\phi} = (1 - \varepsilon)/4$ and $\Delta_{\phi} = (1 - \varepsilon)/3$ with $0 < \varepsilon < 1$. We derive the corresponding β -functions, fixed point values and some observables to one or two-loop order in sections 3.2 and 3.3. These are later compared to numerical results computed using Hamiltonian truncation.

Having built these models in one dimension and derived some perturbative data, we move to the main subject of this work in section 4: Hamiltonian truncation. As the name suggests, this amounts to truncating an otherwise infinite-dimensional Hamiltonian using some scaling dimension cutoff. We start with a 1D CFT whose spectrum is known, given by a Hamiltonian H_0 . We study the theory on a cylinder of unit radius – which acts as an IR regulator – and introduce an interaction term:

$$H = H_0 + \frac{\lambda}{4!} : (\phi_L^4(0) + \phi_R^4(0)) : \quad \text{(LORI)},$$

$$H = H_0 + \frac{ig}{3!} : (\phi_L^3(0) + \phi_R^3(0)) : \quad \text{(LORALY)},$$
(1.5)

where $\phi_{L,R}(0)$ represents the field operator living on the one-dimensional cylinder at a zero-time slice, and n=3 or 4. In order to study these theories at their corresponding conformal fixed points, derived in sections 3.2 and 3.3, we need to impose some conditions on the spectrum:

$$\begin{cases}
\Delta_0 = 0 \\
\Delta_{\partial \phi} = \Delta_{\phi} + 1 \\
\Delta_{\phi^3} = 1 - \Delta_{\phi} \quad \text{(LORI)} \\
\Delta_{\phi^2} = 1 - \Delta_{\phi} \quad \text{(LORALY)}
\end{cases} , \tag{1.6}$$

where the first condition enforces scale invariance of the vacuum, the second ensures the existence of a descendant of ϕ , and the last two are consequences of the equations of motion of LORI and LORALY respectively. Enforcing these conditions requires introducing counter-terms to the Hamiltonian, similarly to usual renormalization in QFT. Incidentally, these conditions can also be enforced in Rayleigh-Schrödinger perturbation theory (see section 4.5), the standard perturbative expansion of introductory quantum mechanics. We derive some perturbative results for LORI to leading order, and in fact for ϕ^{2n} theory for arbitrary n at the fixed point. We subsequently implement the truncation workflow numerically in section 4.6, and find good agreement with some perturbative results.

Lastly, we discuss the construction of effective Hamiltonians for truncation purposes in section 5, which has been addressed in recent work by the community [50–52]. We start by deriving the next-to-leading-order effective Hamiltonian in section 5.1, involving a sum over all heavy states:

$$\langle f|H_{\text{eff}}|i\rangle = \langle f|H_0|i\rangle + \langle f|V|i\rangle + \sum_{\Delta_b > \Delta_T} \frac{\langle f|V|h\rangle\langle h|V|i\rangle}{\Delta_{fh}} + \dots$$
(1.7)

and subsequently demonstrate on a very simple example in LORI that it can drastically improve computations at low UV cutoff Δ_T in section 5.2. We close this discussion by addressing UV divergences in the effective theory (section 5.3), and construct the non-local counter-terms which would in principle cure it of such divergences (sections 5.4, 5.5). We leave the numerical study of these divergences in LORI/LORALY and how to treat them to further work.

2 Construction of LORI and LORALY

2.1 Landau-Ginzburg approach

The long-range models we study here naturally arise from models of interacting Ising spins on a lattice. Consider the corresponding Hamiltonian

$$H[s] = -J \sum_{r \neq r'} \frac{s(r)s(r')}{|r - r'|^{\alpha}} - h \sum_{r} s(r), \qquad (2.1)$$

where h is a uniform external magnetic field and J is some ferromagnetic coupling. The first step in Landau-Ginzburg theory is to replace the study of this lattice model by that of a scalar field ϕ , given by an action of the form

$$S[\phi] = \frac{\mathcal{K}_{\sigma}}{2} \int d^d x d^d x y \frac{\phi(x)\phi(y)}{|x-y|^{d+\sigma}} + \int d^d x \left(\frac{m^2}{2}\phi^2(x) + \frac{g}{3!}\phi^3(x) + \frac{\lambda}{4!}\phi^4(x) + \dots\right). \tag{2.2}$$

where \mathcal{K}_{σ} is some normalization factor. To arrive at this expression, we use a so-called Hubbard-Stratonovich transformation, which amounts to introducing an additional integral over an auxiliary scalar field sourced by the spin fields, and leveraging our knowledge of the Gaussian integral [53]. Defining $J(r-r') \propto |r-r'|^{-\alpha}$ (and ignoring factors of inverse temperature, we'll redefine notations for our final action anyway):

$$Z = \sum_{s(r)} e^{\frac{1}{2} \sum_{r \neq r'} s(r)J(r-r')s(r') + h \sum_{r} s(r)}$$

$$\propto \sum_{s(r)} \int \mathcal{D}[\phi] \exp\left(-\frac{1}{2} \sum_{r \neq r'} \phi(r)J^{-1}(r-r')\phi(r') + \sum_{r} (h+\phi(r))s(r)\right)$$

$$\propto \int \mathcal{D}[\phi] \exp\left(-\frac{1}{2} \sum_{r \neq r'} \phi(r)J^{-1}(r-r')\phi(r') + \sum_{r} \log \cosh (h+\phi(r))\right).$$
(2.3)

Next, we introduce an infinitesimal lattice spacing a in order to take the continuum limit:

$$Z \propto \int \mathcal{D}[\phi] \exp\left(-\frac{1}{2a^{2d}} \int d^dx d^dy \phi(x) J^{-1}(x-y)\phi(y) + \frac{1}{a^d} \int d^dx \log \cosh(h+\phi(x))\right). \tag{2.4}$$

The kinetic term can be further simplified by computing the inverse of $J(x-y) \propto |x-y|^{-\alpha}$. This amounts to finding K such that

$$\int d^d y J(x-y)K(y) = \delta^{(d)}(x-y), \qquad (2.5)$$

Going to momentum space and back (this is akin to the computation in appendix A.1) we arrive at

$$K(x-y) = J^{-1}(x-y) = \int \frac{d^d p}{(2\pi)^d} \frac{e^{-ip(x-y)}}{|p|^{\alpha-d}} \propto \frac{1}{|x-y|^{2d-\alpha}}.$$
 (2.6)

Next, let's look at the interaction terms. They involve an a priori complicated functional $\log \cosh(h + \phi(r))$. By translation invariance, the expectation value of s(r) is independent of r, hence:

$$\langle s \rangle \propto \frac{\partial Z}{\partial h} \propto \langle \tanh(h + \phi) \rangle .$$
 (2.7)

This is reminiscent of the the well-known consistency condition on magnetization in mean field theory, thus we can interpret ϕ as being an order parameter. Hence, as is customary when slightly departing from the mean-field approximation, we can assume the fluctuations of ϕ around its expectation value are small, and subsequently expand the interaction term around $\langle \phi \rangle$:

$$\log \cosh(h + \phi(r)) = g_1 \phi + g_2 \phi^2 + g_3 \phi^3 + g_4 \phi^4 + \dots$$
 (2.8)

As is customary in QFT, we can drop the linear term in ϕ by a field redefinition. Furthermore, the infinite series is typically truncated, since most terms will be irrelevant and won't contribute interesting physics in the IR. Since higher powers are less relevant than lower ones, one doesn't usually look further than the first non-quadratic term. Hence, if we're studying LORI at its second order phase transition – which is a \mathbb{Z}_2 -symmetric theory – we redefine our conventions and arrive at the action

$$S[\phi] = \frac{\mathcal{K}_{\sigma}}{2} \int d^d x d^d x y \frac{\phi(x)\phi(y)}{|x-y|^{d+\sigma}} + \int d^d x \left(\frac{m^2}{2}\phi^2(x) + \frac{\lambda}{4!}\phi^4(x)\right), \qquad (2.9)$$

where setting m=0 for classical conformal invariance leads to our definition of LORI in d dimensions. Another point beside the critical point which is of interest in statistical mechanics is the so-called Lee-Yang edge singularity. This belongs to a locus in parameter space where the partition function vanishes in the disordered phase. It has

been shown that for the Ising model such zeros are located at $h \in i\mathbb{R}$ (this is a special case of a more general result proven in [53–55]). In this case, the most relevant interaction term is

$$\log \cosh(h + \phi(r)) \supset \frac{1}{3} \frac{\tanh h}{\cosh^2 h} \phi^3, \qquad (2.10)$$

which has an imaginary cubic coupling if h is imaginary. We therefore arrive at the following most general action for LORALY:

$$S[\phi] = \frac{\mathcal{K}_{\sigma}}{2} \int d^d x d^d x y \frac{\phi(x)\phi(y)}{|x-y|^{d+\sigma}} + \int d^d x \left(\frac{m^2}{2}\phi^2(x) + \frac{ig}{3!}\phi^3(x)\right), \qquad (2.11)$$

and again we subsequently drop the mass term. Looking at the aforementioned actions in d = 1 dimension yields the models relevant to our study of Hamiltonian truncation in section 4.

Next, let's study an alternative derivation or motivation of these long-range models, which leverages the properties of AdS spacetime and leads directly to a CFT as far as the kinetic part is concerned.

2.2 Construction of long-range theories on the boundary of AdS spacetime

Long-range models in d-dimensions can be obtained from the theory of a massive, local scalar in AdS_{d+1} by integrating out bulk degrees of freedom [56]. Indeed, suppose we start with the following action:

$$S_{\text{AdS}}[\Phi] = \frac{1}{2} \int_{\text{AdS}} dz d^d x \sqrt{-g} \left(g^{AB} \partial_A \Phi \partial_B \Phi + m^2 \Phi^2 \right)$$

$$= \frac{1}{2} \int_{\text{AdS}} dz d^d x l^{d+1} z^{-d-1} \left(l^{-2} z^2 \partial_z \Phi \partial_z \Phi + l^{-2} z^2 \partial^\mu \Phi \partial_\mu \Phi + m^2 \Phi^2 \right) .$$
(2.12)

where the metric is that of a Poincaré patch of an anti-de Sitter space of radius l given by

$$ds^{2} = \frac{l^{2}}{z^{2}} \left(dz^{2} + dx^{\mu} dx_{\mu} \right) . \tag{2.13}$$

To integrate out the bulk, we need the equations of motion of Φ , namely

$$\Box_{\text{AdS}}\Phi = \nabla^A \nabla_A \Phi = \frac{1}{\sqrt{-g}} \partial_A \left(\sqrt{-g} \partial^A \Phi \right) = -m^2 \Phi^2. \tag{2.14}$$

Here,

$$\Box_{\text{AdS}}\Phi = l^{-2}z^2 \left(\partial_z^2 + \partial^\mu \partial_\mu\right) \Phi + l^{-2}(1 - d)z\partial_z\Phi. \tag{2.15}$$

Hence, close to the boundary (dropping the Minkowski spacetime term can be justified by going to Fourier space in x):

$$z^{2}\partial_{z}^{2}\Phi + (1-d)z\partial_{z}\Phi = -m^{2}l^{2}.$$
 (2.16)

This can be solved by a solution of the form $\Phi(z,x)=z^{\Delta}\phi(x)$ such that

$$\Delta(\Delta - d) = -m^2 l^2, \tag{2.17}$$

from which we extract two roots Δ_{\pm} such that $\Delta_{-} < \Delta_{+}$ and

$$\Phi(z,x) \underset{z \to 0}{\sim} z^{\Delta_{-}} \phi(x). \tag{2.18}$$

We can conveniently integrate out the $\{\Phi(z,x)\}_{z>0}$ in (2.12) by introducing a bulk-to-boundary propagator K(z,x) [57] such that

$$\Phi(z,x) = \int d^d y K(z,x-y)\phi(x), \qquad (2.19)$$

with K satisfying

$$\begin{cases} (\Box_{\text{AdS}} + m^2) K(z, x) \\ K(z, x) \underset{z \to 0}{\sim} z^{\Delta -} \delta^{(d)}(x) \end{cases}$$
 (2.20)

¹Greek indices indicate contraction with respect to the Minkowski metric in this section.

The next step is to substitute (2.19) into (2.12). Using integration by parts, we have the following expression on-shell

$$S_{\text{AdS}}[\phi] \sim \frac{l^{d-1}}{2z^{d-1}} z^{\Delta_{-}} \int_{z \to 0} d^d x d^d y \phi(x) \phi(y) \partial_z K(z, x - y) \,.$$
 (2.21)

It can subsequently be shown that the appropriate expression for K is [57]

$$K(z,x) = \frac{Cz^{\Delta_{+}}}{(z^{2} + x^{2})^{\Delta_{+}}}.$$
 (2.22)

This leads to

$$S_{\partial AdS}[\phi] = \frac{\mathcal{K}_{\sigma}}{2} \int d^d x d^d y \frac{\phi(x)\phi(y)}{|x-y|^{d+\sigma}} = \frac{1}{2} \int d^d x \phi(x) \mathcal{L}_{\sigma}\phi(y).$$
 (2.23)

where we define $\sigma = 2\Delta_- - d$. Note that we've introduced some normalization \mathcal{K}_{σ} related to the fractional Laplacian \mathcal{L}_{σ}^2 . This is a theory on the boundary of AdS_{d+1} , which we know to be conformal to $\mathbb{R} \times S^{d-1}$. This takes care of the kinetic part of long-range theories. As for monomial interactions, they can be obtained by simply introducing a boundary term to the action (2.12) of the form $g_0 \int d^d x \Phi(0, x)^n$.

2.3 Theories on the cylinder

This work deals with one-dimensional models, let's specialize the action (2.23) to d=1. Since the boundary ∂AdS_2 of two-dimensional anti-de Sitter space is conformal to a one-dimensional cylinder $\mathbb{R} \times S^0$, let's use a plane-cylinder map $|x| = e^{\tau}$. The action (2.23) describes a CFT, therefore we know that under such a map, the primary field ϕ transforms as

$$\phi(x) = \begin{cases} e^{-\Delta_{\phi}\tau} \phi_L(\tau) & \text{if } x < 0 \\ e^{-\Delta_{\phi}\tau} \phi_R(\tau) & \text{if } x > 0 \end{cases}$$
 (2.24)

where L, R refer to the 'left' or 'right' copy of \mathbb{R} constituting the one-dimensional cylinder, and $\Delta_{\phi} = (d - \sigma)/2$ (see appendix A.1). This leads to

$$S_{0}[\phi] = \frac{\mathcal{K}_{\sigma}}{2^{3-2\Delta_{\phi}}} \int d\tau_{1} d\tau_{2} \frac{\phi_{L}(\tau_{1})\phi_{L}(\tau_{2})}{|\sinh\left(\frac{\tau_{1}-\tau_{2}}{2}\right)|^{2(1-\Delta_{\phi})}} + \frac{\mathcal{K}_{\sigma}}{2^{3-2\Delta_{\phi}}} \int d\tau_{1} d\tau_{2} \frac{\phi_{R}(\tau_{1})\phi_{R}(\tau_{2})}{|\sinh\left(\frac{\tau_{1}-\tau_{2}}{2}\right)|^{2(1-\Delta_{\phi})}} + \frac{\mathcal{K}_{\sigma}}{2^{2(1-\Delta_{\phi})}} \int d\tau_{1} d\tau_{2} \frac{\phi_{L}(\tau_{1})\phi_{R}(\tau_{2})}{\cosh\left(\frac{\tau_{1}-\tau_{2}}{2}\right)^{2(1-\Delta_{\phi})}}.$$
(2.25)

Hence, in the free theory on the cylinder, the fields on each connected component, namely a copy of \mathbb{R} , are correlated with one another. Upon including ϕ^n interactions, we arrive at

$$S[\phi] = S_0[\phi] + \frac{g_0}{n!} \int d\tau \left[\phi_L^n(\tau) + \phi_R^n(\tau) \right] , \qquad (2.26)$$

where for n=4 we recover classical LORI, and for n=3 and an imaginary coupling we recover classical LORALY. However, since we want our theory to be conformally invariant at the quantum level, we need to derive the corresponding conformal fixed points. We can subsequently derive some observables, which will prove useful to the study of Hamiltonian truncation and ascertaining its validity at weak coupling.

3 Renormalization group analysis

3.1 Preliminary remarks and a comment regarding non-locality

The generalized free field ϕ involved in the long-range models introduced in the previous section has scaling dimension $\Delta_{\phi} = (d - \sigma)/2$, which entails that the quartic and cubic couplings respectively have dimensions

$$[\lambda] = d - 4\Delta_{\phi} = 2\sigma - d, \qquad (3.1)$$

$$[g] = d - 3\Delta_{\phi} = \frac{3\sigma - d}{2}. \tag{3.2}$$

Classically, it suffices to take $\sigma = d/2$ or $\sigma = d/3$ to have a conformally invariant LORI or LORALY. However, quantum corrections might break scale invariance. In order to recover conformally invariant theories in the IR, we

²More precisely, the fractional Laplacian is defined so as to satisfy $\mathcal{L}_{\sigma}e^{ipx} = |p|^{\sigma}e^{ipx}$.

need to derive the corresponding β -functions. To do so, we use an ε -expansion to render the couplings marginally relevant, which triggers an RG flow to the IR. One way to do this is to fix the dimension d, and work with σ such that $[\lambda] = \varepsilon$ or $[g] = \varepsilon$:

$$\Delta_{\phi} = \frac{d - \varepsilon}{4}, \quad \sigma = \frac{d + \varepsilon}{4} \quad \text{(LORI)};$$
(3.3)

$$\Delta_{\phi} = \frac{d - \varepsilon}{3}, \quad \sigma = \frac{d + 2\varepsilon}{3} \quad (LORALY).$$
(3.4)

With these choices, divergences will appear from one-loop order and onwards. These can be absorbed by introducing counter-terms to the initial actions. Concretely, we define renormalization factors Z_{ϕ} , Z_{λ} , Z_{q} such that:

$$g_0 = Z_q g \mu^{\varepsilon}, \quad \lambda_0 = Z_{\lambda} \lambda \mu^{\varepsilon}, \quad \phi = Z_{\phi}[\phi]$$
 (3.5)

where the two μ^{ε} factors above are not the same since pertaining to distinct theories, but are merely here to remind the reader of the dimensionality of the couplings in the ε -expansion. Note that wavefunction renormalization would introduce a non-local counter-term to the bare action, i.e. in momentum space we would have a counter-term $\sim \delta_{\phi}\phi(-p)|p|^{\sigma}\phi(p)$ for a non-integer σ in general. However, UV divergences are always local, meaning that in momentum space they only involve integer powers of external momentum p. Indeed, UV divergences stem from the behavior of loop corrections at high loop momentum, where external momentum p can be treated as small and the relevant diagrams can be Taylor-expanded near p=0 and thus generate integer powers of p. As a simple check, let's examine the lowest non-trivial loop order amputated contributions to the two-point function in both LORI and LORALY:

$$= \frac{\lambda_0^2}{6} \int \frac{d^d k}{(2\pi)^d} \frac{d^d l}{(2\pi)^d} \frac{1}{|k|^{\sigma} |k+l+p|^{\sigma} |l|^{\sigma}} = \frac{\lambda_0^2}{6(2\pi)^{2d}} \frac{w_{\sigma}^3}{w_{3\sigma-2d}} \frac{1}{|p|^{3\sigma-2d}}$$

$$= \frac{\lambda_0^2}{6(4\pi)^d} \frac{\Gamma\left(-\frac{d}{4}\right)}{\Gamma\left(\frac{3d}{4}\right)} |p|^{\frac{d}{2}} + O(\varepsilon) \quad \text{(LORI)},$$
(3.6)

$$- \frac{g_0^2}{2} \int \frac{d^d k}{(2\pi)^d} \frac{1}{|k|^{\sigma}|k+p|^{\sigma}} = -\frac{g_0^2}{2(2\pi)^d} \frac{w_\sigma^2}{w_{2\sigma-d}} \frac{1}{|p|^{2\sigma-d}}$$

$$= -\frac{g_0^2}{2(4\pi)^{\frac{d}{2}}} \frac{\Gamma\left(-\frac{d}{6}\right) \Gamma\left(\frac{d}{3}\right)^2}{\Gamma\left(\frac{d}{6}\right)^2 \Gamma\left(\frac{2d}{3}\right)} |p|^{\frac{d}{3}} + O(\varepsilon) \quad \text{(LORALY)}.$$

$$(3.7)$$

Notice that for generic d, neither of these expressions diverge as $\varepsilon \to 0$. However, interestingly enough, if we also conduct an ε -expansion in d, namely take $d = 4 - \hat{\varepsilon}$ for LORI and $d = 6 - \hat{\varepsilon}$ for LORALY with $\hat{\varepsilon}$ a new infinitesimal parameter, then these diagrams do diverge. This is due to the fact that as one approaches d = 4 (resp. d = 6) for LORI (resp. LORALY), $\sigma \to 2$, $\mathcal{L}_{\sigma} \to -\partial^2$ and we subsequently recover local ϕ^4 (resp. ϕ^3) theory. In this regime, it is consistent to have wavefunction renormalization, since the kinetic counter-term becomes local. Such an expansion was conducted to study the localized magnetic field and the surface defect in LORI close to d = 4 in [58] for example.

Since we'll be working in d=1, the bare two-point function will always be finite and we can assume $Z_{\phi}=1$, i.e. that the bare ϕ and renormalized $[\phi]$ coincide. As is customary in CFT, let's choose a field normalization which yields $\langle \phi(x)\phi(y)\rangle = |x-y|^{-2\Delta_{\phi}}$ exactly. The kernel of the fractional Laplacian is given by

$$G(x-y) = \frac{2^{d-\sigma}\Gamma\left(\frac{d-\sigma}{2}\right)}{(4\pi)^{\frac{d}{2}}\Gamma\left(\frac{\sigma}{2}\right)} \frac{1}{|x-y|^{2\Delta_{\phi}}} = \frac{\mathcal{N}_{\sigma}}{|x-y|^{2\Delta_{\phi}}},$$
(3.8)

as explained in appendix A.1. Hence, in what follows, we'll therefore always be working with the primary operator $\tilde{\phi} := \phi/\sqrt{N_{\sigma}}$, and we'll make no distinction between ϕ and $\tilde{\phi}$. Now that we've fully taken care of the two-point function, let's turn to the renormalization of the vertex and the derivation of some loop-corrected scaling dimensions in sections 3.2 and 3.3. To this effect, we also refer the reader to appendix A for all of the basic reminders, conventions and computations needed for what follows.

3.2 ε -expansion for LORI

In this subsection and the next, we derive the CFT data in the ε -expansion for LORI which will be useful to our study of Hamiltonian truncation in section 4. This requires we start by deriving the Wilson-Fisher fixed point at which we compute our observables, which stems from the renormalization of the quartic vertex. Up to our choices

of convention and the non-local nature of LORI, this story follows the usual treatment of $\lambda \phi^4$ theory (see [59] for a comprehensive review).

3.2.1 Two-loop renormalization of the vertex

Let's turn to the two-loop renormalization of the quartic coupling λ . To this end, we introduce the counter-term interaction

$$= -\left(\frac{a\lambda^2 + b\lambda^3}{\varepsilon} + \frac{c\lambda^3}{\varepsilon^2}\right)\mu^{\varepsilon}, \tag{3.9}$$

where a, b, c are constants which will be fixed to cancel divergences incurred in the two-loop corrections to the vertex. These corrections are given by the following Feynman diagrams, which are computed using the convolution formula derived in appendix A.2:

$$= \frac{3\lambda^2 \mu^{2\varepsilon}}{2\mathcal{N}_{\sigma}^2 (2\pi)^d} \frac{w_{\sigma}^2}{w_{2\sigma-d}} \frac{1}{|p|^{2\sigma-d}} = \frac{3\pi^{\frac{d}{2}}\lambda^2}{\Gamma(\frac{d}{2})\varepsilon} + O(\varepsilon^0),$$
 (3.10)

$$= -\frac{3\lambda^{3}\mu^{3\varepsilon}}{4\mathcal{N}_{\sigma}^{4}(2\pi)^{2d}} \frac{w_{\sigma}^{4}}{w_{2\sigma-d}^{2}} \frac{1}{|p|^{4\sigma-2d}}$$

$$= -\frac{3\pi^{d}\lambda^{3}}{\Gamma\left(\frac{d}{2}\right)^{2}\varepsilon} \left(\frac{1}{\varepsilon} - \gamma + 2\log 2 + \psi\left(\frac{d}{2}\right)\right) + O\left(\varepsilon^{0}, \log\left|\frac{p}{\mu}\right|\right),$$
(3.11)

$$= -\frac{3\lambda^{3}\mu^{3\varepsilon}}{\mathcal{N}_{\sigma}^{4}(2\pi)^{2d}} \frac{w_{\sigma}^{3}w_{3\sigma-d}}{w_{2\sigma-d}w_{4\sigma-2d}} \frac{1}{|p|^{4\sigma-2d}}$$

$$= -\frac{3\pi^{d}\lambda^{3}}{\Gamma\left(\frac{d}{2}\right)^{2}\varepsilon} \left(\frac{2}{\varepsilon} - 3\gamma + 4\log 2 - 2\psi\left(\frac{d}{4}\right) + 3\psi\left(\frac{d}{2}\right)\right) + O\left(\varepsilon^{0}, \log\left|\frac{p}{\mu}\right|\right),$$
(3.12)

$$= \frac{3a\lambda^{3}\mu^{2\varepsilon}}{\mathcal{N}_{\sigma}^{2}(2\pi)^{d}\varepsilon} \frac{w_{\sigma}^{2}}{w_{2\sigma-d}} \frac{1}{|p|^{2\sigma-d}} = \frac{3a\pi^{\frac{d}{2}}\lambda^{3}}{\Gamma\left(\frac{d}{2}\right)\varepsilon} \left(\frac{2}{\varepsilon} - \gamma - 2\log 2 + \psi\left(\frac{d}{2}\right)\right) + O\left(\varepsilon^{0}, \log\left|\frac{p}{\mu}\right|\right).$$
 (3.13)

Incidentally, we've dropped momentum-dependent terms since they are not needed for computing the coupling renormalization factor. That being said, terms involving poles in ε and momentum simultaneously should vanish in the full two-loop correction. Renormalization conditions – in the MS scheme used throughout this section – lead to

$$a = \frac{3\pi^{\frac{d}{2}}}{\Gamma\left(\frac{d}{2}\right)}, \quad b = -\frac{3\pi^{d}}{\Gamma\left(\frac{d}{2}\right)^{2}} \left(\psi\left(\frac{d}{2}\right) - 2\psi\left(\frac{d}{4}\right) - \gamma\right), \quad c = \frac{9\pi^{d}}{\Gamma\left(\frac{d}{2}\right)^{2}} = a^{2}.$$
(3.14)

Hence, to two-loop order, we introduce the coupling renormalization factor:

$$Z_{\lambda} = 1 + \frac{3}{\Gamma\left(\frac{d}{2}\right)} \frac{\lambda}{\varepsilon} \frac{\lambda}{(4\pi)^{\frac{d}{2}}} + \frac{3\lambda^{2}}{(4\pi)^{d}\Gamma\left(\frac{d}{2}\right)^{2}} \left(\frac{3}{\varepsilon^{2}} - \frac{\psi\left(\frac{d}{2}\right) - 2\psi\left(\frac{d}{4}\right) - \gamma}{\varepsilon}\right) + O(\lambda^{3}), \tag{3.15}$$

where ψ is the logarithmic derivative of the Γ -function, known as the digamma function. We finally arrive at the following β -function, which agrees with expressions quoted in [60, 61]:

$$\beta_{\lambda}(\lambda) = -\varepsilon \lambda + \frac{3\pi^{\frac{d}{2}}}{\Gamma\left(\frac{d}{2}\right)} \lambda^{2} - \frac{6\pi^{d}(\psi\left(\frac{d}{2}\right) - 2\psi\left(\frac{d}{4}\right) - \gamma)}{\Gamma\left(\frac{d}{2}\right)^{2}} \lambda^{3} + O\left(\lambda^{4}\right). \tag{3.16}$$

³The condition $c = a^2$ is a good consistency check for ensuring our computations are correct, otherwise the β -function has a pole in ε .

3.2.2 Fixed point and anomalous dimension of ϕ^4 to two-loop order

This β -function has a non-trivial zero, the so-called Wilson-Fisher fixed point:

$$\lambda_* = \frac{\Gamma\left(\frac{d}{2}\right)}{3\pi^{\frac{d}{2}}} \left[\varepsilon + \frac{2\left(\psi\left(\frac{d}{2}\right) - 2\psi\left(\frac{d}{4}\right) - \gamma\right)}{3} \varepsilon^2 + O\left(\varepsilon^2\right) \right]. \tag{3.17}$$

The theory at $\lambda = \lambda_*$ is scale-invariant by construction. Moreover, it has been shown to be conformally invariant in [56], as reviewed in [62, 63]. Therefore, in one dimension we can legitimately call LORI a 1D CFT, provided we take

$$\lambda = \lambda_* = \frac{\varepsilon}{3} + 1.31426\varepsilon^2 + O(\varepsilon^3). \tag{3.18}$$

It's worth noting that the above β -function yields a CFT datum for free (see appendix C for proof of the general statement):

$$\Delta_{\phi^4} = d + \frac{\partial \beta_{\lambda}}{\partial \lambda} \bigg|_{\lambda = \lambda_{\alpha}} = d + \varepsilon - \frac{2\left(\psi\left(\frac{d}{2}\right) - 2\psi\left(\frac{d}{4}\right) - \gamma\right)}{3}\varepsilon^2 + O\left(\varepsilon^3\right). \tag{3.19}$$

Hence, in one dimension ⁴:

$$\Delta_{\phi^4} = 1 + \varepsilon - 2.94279\varepsilon^2 + O(\varepsilon^3). \tag{3.20}$$

3.2.3 Anomalous dimension of ϕ^2 to two-loop order

Another often quoted observable that will be useful for our purposes is the anomalous dimension of ϕ^2 . In practice, it might also be computed more accurately with Hamiltonian truncation than Δ_{ϕ^4} , which is closer to the UV cutoff. The relevant tree level, one-loop and two-loop diagrams are

$$\phi^2 \qquad \qquad \phi^2 = \frac{2}{|x|^{4\Delta_\phi}}, \qquad (3.21)$$

$$\phi^2 \left(\frac{\lambda^2 \mu^{2\varepsilon}}{2} \frac{w_{4\Delta_{\phi}}^3}{w_{12\Delta_{\phi}-2d}} \frac{1}{|x|^{12\Delta_{\phi}-2d}}, \right. \tag{3.23}$$

$$\phi^2 \left(\bigcap \right) \phi^2 \supset 2\lambda^2 \left(-\frac{2\pi^{\frac{d}{2}}}{\Gamma\left(\frac{d}{2}\right)} \varepsilon \frac{w_{4\Delta_{\phi}} w_{2\Delta_{\phi}}}{w_{6\Delta_{\phi}-d}} \frac{1}{|x|^{4\Delta_{\phi}}} + \frac{w_{2\Delta_{\phi}} w_{4\Delta_{\phi}}^2 w_{8\Delta_{\phi}-d}}{w_{6\Delta_{\phi}-d} w_{12\Delta_{\phi}-2d}} \frac{1}{|x|^{12\Delta_{\phi}-2d}} \right), \tag{3.24}$$

where the last diagram is the most challenging to evaluate exactly, and we've instead extracted its divergence in appendix B.1. Canceling the corresponding poles in the renormalized theory requires the introduction of a renormalization factor for ϕ^2 :

$$Z_{\phi^2} = 1 - \frac{\pi^{\frac{d}{2}}}{\Gamma\left(\frac{d}{2}\right)} \frac{\lambda}{\varepsilon} - \frac{\pi^d \left(\gamma + 2\psi\left(\frac{d}{4}\right) - \psi\left(\frac{d}{2}\right)\right)}{2\Gamma\left(\frac{d}{2}\right)^2} \frac{\lambda^2}{\varepsilon} - \frac{\pi^d}{\Gamma\left(\frac{d}{2}\right)^2} \frac{\lambda^2}{\varepsilon^2}, \tag{3.25}$$

yielding the following scaling dimension at two loops:

$$\Delta_{\phi^2} = \frac{d - \varepsilon}{2} + \frac{d \log Z_{\phi^2}}{d \log \mu} \bigg|_{\lambda = \lambda_*} = \frac{d}{2} - \frac{\varepsilon}{6} + \frac{1}{9} \left(-\gamma - 2\psi \left(\frac{d}{4} \right) + \psi \left(\frac{d}{2} \right) \right) \varepsilon^2 + O(\varepsilon^3). \tag{3.26}$$

This is the expression used in [61]. In one dimension, the relevant expression is therefore

$$\Delta_{\phi^2} = \frac{1}{2} - \frac{\varepsilon}{6} + 0.657131\varepsilon^2 + O(\varepsilon^3). \tag{3.27}$$

⁴Note that we'll be a little loose with significant figures for the purpose of this report. A more systematic approach would require being more careful when quoting these results.

3.2.4 Anomalous dimension of ϕ^n to one-loop order

If we decrease our tolerance regarding loop orders, say merely addressing one-loop expansions, then we can say a lot more. Namely, we can derive the anomalous dimensions of all composite operators ϕ^n . Consider the following diagrams at tree and one-loop level:

$$\phi^n = \frac{n!}{|x|^{2n\Delta_\phi}}, \tag{3.28}$$

$$\phi^{n} = -\frac{n! n(n-1)\lambda \mu^{\varepsilon}}{4} \frac{w_{4\Delta_{\phi}}^{2}}{w_{8\Delta_{\phi}-d}} \frac{1}{|x|^{(8+2n-4)\Delta_{\phi}-d}}.$$
 (3.29)

The second diagram diverges, and we can introduce the wavefunction renormalization

$$Z_{\phi^n} = 1 - \frac{n(n-1)\pi^{\frac{d}{2}}}{2\Gamma\left(\frac{d}{2}\right)} \frac{\lambda}{\varepsilon} + O(\lambda^2).$$
(3.30)

which leads to the scaling dimension

$$\Delta_{\phi^n} = \frac{nd}{4} + \frac{n(2n-5)}{12}\varepsilon + O(\varepsilon^2). \tag{3.31}$$

3.3 ε -expansion for LORALY

Next, let's derive perturbative results for LORALY. Some of these results can be cross-checked with statements regarding local ϕ^3 theory from [64–66].

3.3.1 Two-loop renormalization of the vertex

Let's renormalize the three-point vertex. To simplify computations, let's take external momenta p_1, p_2, p_3 such that $p_2 = -p_1$ and $p_3 = p_1 + p_2 = 0$. The relevant diagrams at tree, one-loop and two-loop levels are

$$=-ig\mu^{\varepsilon}\,, (3.32)$$

$$= \frac{ig^{3}\mu^{3\varepsilon}}{(2\pi)^{d}\mathcal{N}_{\sigma}^{3}} \frac{w_{2\sigma}w_{\sigma}}{w_{3\sigma-d}} \frac{1}{|p|^{3\sigma-d}}$$

$$= \frac{ig^{3}\pi^{d}\Gamma\left(\frac{d}{6}\right)^{3}}{\Gamma\left(\frac{d}{3}\right)^{3}\Gamma\left(\frac{d}{2}\right)} \left(\frac{1}{\varepsilon} - \gamma + 2\log 2 + \psi\left(\frac{d}{2}\right)\right) + O\left(\varepsilon, \log\left|\frac{p}{\mu}\right|\right),$$
(3.33)

$$= -\frac{3ig^{5}\mu^{5\varepsilon}}{(2\pi)^{2d}\mathcal{N}_{\sigma}^{6}} \frac{w_{\sigma}^{2}w_{2\sigma}w_{5\sigma-d}}{w_{3\sigma-d}w_{6\sigma-2d}} \frac{1}{|p|^{6\sigma-2d}}$$

$$= -\frac{3ig^{5}\pi^{2d}\Gamma\left(\frac{d}{6}\right)^{6}}{2\Gamma\left(\frac{d}{3}\right)^{6}\Gamma\left(\frac{d}{2}\right)^{2}\varepsilon} \left(\frac{1}{\varepsilon} - 3\gamma + 4\log 2 - \psi\left(\frac{d}{6}\right) - \psi\left(\frac{d}{3}\right) + 3\psi\left(\frac{d}{2}\right)\right) + O\left(\varepsilon, \log\left|\frac{p}{\mu}\right|\right),$$
(3.34)

$$= -\frac{ig^5 \mu^{5\varepsilon}}{4(2\pi)^{2d} \mathcal{N}_{\sigma}^6} \frac{w_{2\sigma}^2}{w_{4\sigma-d}} \frac{\pi^{\frac{d}{2}}}{\Gamma\left(\frac{d}{2}\right)\varepsilon} = \frac{-ig^5 \pi^{2d} \Gamma\left(\frac{d}{6}\right)^9}{4\Gamma\left(\frac{d}{3}\right)^9 \Gamma\left(\frac{d}{2}\right)\varepsilon} + O\left(\varepsilon, \log\left|\frac{p}{\mu}\right|\right),$$
 (3.35)

The relevant counter-terms are of the form

$$= -i\left(g + \frac{ag^3 + bg^5}{\varepsilon} + \frac{cg^5}{\varepsilon^2}\right)\mu^{\varepsilon}, \qquad (3.36)$$

$$= \frac{3iag^5 \mu^{3\varepsilon} \pi^d \Gamma\left(\frac{d}{6}\right)^3}{\Gamma\left(\frac{d}{3}\right)^3 \Gamma\left(\frac{d}{2}\right) \varepsilon} \left(\frac{1}{\varepsilon} - \gamma + 2\log 2 + \psi\left(\frac{d}{2}\right)\right) + O\left(\varepsilon, \log\left|\frac{p}{\mu}\right|\right),$$
 (3.37)

where a, b, c are to be tuned to cancel divergences. To cancel poles in the MS scheme, one must take⁵

$$a = \frac{\pi^d \Gamma\left(\frac{d}{6}\right)^3}{\Gamma\left(\frac{d}{3}\right)^3 \Gamma\left(\frac{d}{2}\right)},\tag{3.38}$$

$$b = -\frac{\pi^{2d}\Gamma\left(\frac{d}{6}\right)^{6}}{4\Gamma\left(\frac{d}{6}\right)^{9}\Gamma\left(\frac{d}{6}\right)^{3}\Gamma\left(\frac{d}{2}\right) - 6\Gamma\left(\frac{d}{3}\right)^{3}\left(\gamma + \psi\left(\frac{d}{6}\right) + \psi\left(\frac{d}{3}\right) - \psi\left(\frac{d}{2}\right)\right)\right), \tag{3.39}$$

$$c = \frac{3}{2} \frac{\pi^{2d} \Gamma\left(\frac{d}{6}\right)^6}{\Gamma\left(\frac{d}{3}\right)^6 \Gamma\left(\frac{d}{2}\right)^2}.$$
(3.40)

Requiring scale invariance of the bare coupling leads to the β -function of LORALY:

$$\beta(g) = -\varepsilon g + \frac{2\pi^d \Gamma\left(\frac{d}{6}\right)^3}{\Gamma\left(\frac{d}{3}\right)^3 \Gamma\left(\frac{d}{2}\right)} g^3 - \frac{\pi^{2d} \Gamma\left(\frac{d}{6}\right)^6 \left(\Gamma\left(\frac{d}{6}\right)^3 \Gamma\left(\frac{d}{2}\right) - 6\Gamma\left(\frac{d}{3}\right)^3 \left(\gamma + \psi\left(\frac{d}{6}\right) + \psi\left(\frac{d}{3}\right) - \psi\left(\frac{d}{2}\right)\right)\right)}{\Gamma\left(\frac{d}{3}\right)^9 \Gamma\left(\frac{d}{2}\right)^2} g^5 + O(g^7) \,. \tag{3.41}$$

3.3.2 Fixed point and anomalous dimension of ϕ^3 to two-loop order

We can subsequently derive the non-trivial fixed point

$$g_*^2 = \frac{\Gamma\left(\frac{d}{2}\right)\Gamma\left(\frac{d}{3}\right)^3}{2\pi^d\Gamma\left(\frac{d}{6}\right)^3}\varepsilon + \frac{\Gamma\left(\frac{d}{2}\right)}{8\pi^d\Gamma\left(\frac{d}{6}\right)^3}\left[\Gamma\left(\frac{d}{6}\right)^3\Gamma\left(\frac{d}{2}\right) - 6\Gamma\left(\frac{d}{3}\right)^3\left(\gamma + \psi\left(\frac{d}{6}\right) + \psi\left(\frac{d}{3}\right) - \psi\left(\frac{d}{2}\right)\right)\right]\varepsilon^2 + O(\varepsilon^3)\,, \eqno(3.42)$$

which in one dimension is given by

$$q_{*}^{2} = 0.031447\varepsilon + 0.451582\varepsilon^{2} + O(\varepsilon^{3}). \tag{3.43}$$

It bears mentioning that the factor of i in the LORALY coupling is responsible for the existence of this non-trivial real fixed point, and it is an *ad hoc* justification for studying LORALY in the context of 1D CFTs. The scaling dimension of ϕ^3 is again derived using the same derivative trick as in 3.2.2:

$$\Delta_{\phi^3} = d + 2\varepsilon + \left[-\frac{\Gamma\left(\frac{d}{6}\right)^3 \Gamma\left(\frac{d}{2}\right)}{2\Gamma\left(\frac{d}{3}\right)^3} + 3\left(\gamma + \psi\left(\frac{d}{6}\right) + \psi\left(\frac{d}{3}\right) - \psi\left(\frac{d}{2}\right)\right) \right] \varepsilon^2 + O(\varepsilon^3), \tag{3.44}$$

which, in one dimension, reads

$$\Delta_{\phi^3} = 1 + 2\varepsilon - \left(2\sqrt{3}\pi + \frac{2\pi^2}{\Gamma\left(\frac{2}{3}\right)^3} + 9\log 3\right)\varepsilon^2 + O(\varepsilon^3) \sim 1 + 2\varepsilon - 28.7202\varepsilon^2 + O(\varepsilon^3). \tag{3.45}$$

Note that this agrees with local ϕ^3 theory at one-loop [64].

3.3.3 Anomalous dimension of ϕ^n to one-loop order

While quite involved at two-loops, the computation of the anomalous dimension of ϕ^n at one-loop order is a fairly straightforward generalization of the computation conducted in appendix B.2. Indeed we can generalize the diagram computations for ϕ^4 to the case of ϕ^n for any $n \geq 4$, since this just adds additional legs connecting the external vertices.

$$\phi^n \longrightarrow \frac{n^2(n-1)^2(n-2)!g^2\pi^{\frac{d}{2}}w_{2\Delta_{\phi}}^2}{\Gamma\left(\frac{d}{2}\right)w_{4\Delta_{\phi}-d}}\frac{1}{\varepsilon}\frac{1}{|x|^{8\Delta_{\phi}}},\tag{3.46}$$

⁵Important consistency check: must have $c = 3a^2/2$ otherwise $\beta(g)$ has a pole in ε .

This yields the following one-loop renormalization factor and scaling dimension for all ϕ^n composite operators:

$$Z_{\phi^n} = 1 - \frac{n(n-1)\pi^d \Gamma\left(\frac{d}{6}\right)^3}{2\Gamma\left(\frac{d}{2}\right)^3 \Gamma\left(\frac{d}{2}\right)} \frac{g^2}{\varepsilon} + O(g^3)$$
(3.47)

$$\Delta_{\phi^n} = \frac{nd}{3} + \frac{(3n-5)n}{6}\varepsilon + O(\varepsilon^2). \tag{3.48}$$

4 Hamiltonian truncation

4.1 Setup

Now that we've developed a reasonably solid understanding of the models at hand, and derived some observables perturbatively, let's turn to the study of Hamiltonian truncation for our long-range one-dimensional CFTs. Consider a QFT in a finite volume, whose Hamiltonian is defined at a given time slice by

$$H = H_0 + V \,, \tag{4.1}$$

where H_0 is a Hamiltonian whose spectrum is known, and V is a deforming term. Since we're not working in d=2, where we would have access to a plethora of solvable CFTs to use for H_0 , we start from a free theory. We then add an interacting contribution weighted by a coupling constant g. In order to handle potential IR divergences, let's also place this theory on a cylinder of unit radius, with the infinite direction corresponding to time:

$$H = H_0 + g \int d^{d-1}x \mathcal{O}(0, \vec{x}). \tag{4.2}$$

In general, one also takes H_0 to have a discrete spectrum. This will hold in our case since H_0 describes a free field in a finite volume, for which periodic boundary conditions in the spatial direction on the cylinder lead to discrete energy levels. In this work, we always assume H_0 to be the Hamiltonian of a generalized free field (GFF) ϕ , which is the quantum analogue of the classical Hamiltonian derived in section 2.2. This Hamiltonian is constructed using radial quantization, reviewed for our setup in section 4.3, and as such the relevant Hilbert space \mathcal{H} is a Fock space spanned by the eigenbasis of H_0 :

$$|\vec{k}\rangle = |k_0, k_1, \dots, k_n, \dots\rangle := \prod_{i=0}^{\infty} \left[\partial^i \phi(0)\right]^{k_i} |0\rangle, \quad (k_i) \in \mathbb{N}^{\mathbb{N}},$$

$$(4.3)$$

where k_i is an occupation number in the *i*-th position of the state vector, corresponding to the *i*-th mode. Indeed, we've promoted the GFF ϕ to an operator which can act on a vacuum to produce states on the cylinder, in accordance with the state-operator correspondence in CFT, which we review in section 4.2 for completeness. The spectrum of H_0 is obtained from the eigenvalue equations:

$$H_0|\vec{k}\rangle = \sum_{l=0}^{\infty} k_l \left(\Delta_{\phi} + l\right) |\vec{k}\rangle. \tag{4.4}$$

Next, in principle we need to evaluate the matrix elements of the interaction Hamiltonian V in this basis. This will give us the full Hamiltonian H, which we subsequently want to diagonalize to solve our theory. This is naturally very costly and usually unfeasible. Hamiltonian truncation amounts instead to picking a cutoff Δ_T such that we discard all states of energy $\Delta > \Delta_T$ in the free theory. This is tantamount to separating out the full Hilbert space \mathcal{H} into light and heavy subspaces such that $\mathcal{H} = \mathcal{H}_l \oplus \mathcal{H}_h$, and replacing the diagonalization of the full Hamiltonian by that of H restricted to $\mathcal{H}_{\text{eff}} := \mathcal{H}_l$. Denoting the truncated Hamiltonian H_{eff} , a reasonable expectation is that for Δ_T large enough:

$$\forall |i\rangle, |j\rangle \in \mathcal{H}_{\text{eff}}, \langle i|H_{\text{eff}}|j\rangle \approx \langle i|H|j\rangle$$
 (4.5)

and that the low-lying spectrum is reproduced faithfully. This expectation is satisfied to a certain extent, as our numerics show in the case of LORI and LORALY in 4.6. Throughout this section, we study the two following Hamiltonians

$$H = H_0 + \frac{\lambda}{4!} : \left(\phi_L^4(0) + \phi_R^4(0)\right) :, \tag{4.6}$$

$$H = H_0 + \frac{ig}{3!} : \left(\phi_L^3(0) + \phi_R^3(0)\right) :, \tag{4.7}$$

where $\phi_{L,R}(0)$ represents the field operator living on the one-dimensional cylinder at a zero-time slice. Before moving on to radial quantization, one might be concerned that working on the cylinder fundamentally changes the physics we are studying, and hence yields incorrect predictions for physical quantities in the corresponding QFT in \mathbb{R}^d or $\mathbb{R}^{1,d-1}$. Provided we do things carefully, this is not an issue (the argument which follows is adapted from [30]). Indeed, suppose we start on the plane, where the theory is described by H, which has cubic and quartic couplings g_3, g_4 and has a continuous spectrum. Normal-ordering tells us that

$$: \phi^4 := \phi^4 - 6Z\phi^2 + 3Z^2, \quad : \phi^3 := \phi^3 - 3Z\phi, \tag{4.8}$$

where Z is a tadpole integral corresponding to a self-contraction. On the cylinder, we have equivalent expressions, except with a different factor z:

$$: \phi_{\text{cvl}}^4 := \phi^4 - 6z\phi^2 + 3z^2, \quad : \phi_{\text{cvl}}^3 := \phi^3 - 3z\phi. \tag{4.9}$$

To go from H on the plane to H_{cyl} on the cylinder, we need to account for the change in normal-ordering counterterms:

$$H_{\text{cyl}} = H - 6g_4(z - Z)\phi^2 + 3g_4(z^2 - Z^2) - 3g_3(z - Z)\phi_{\text{cyl}}$$

= $H - 6g_4(z - Z) : \phi_{\text{cyl}}^2 : -3g_4(z - Z)^2 - 3g_3(z - Z)\phi_{\text{cyl}}.$ (4.10)

The term linear in ϕ merely shifts the VEV of ϕ , and hence we can discard it by redefining our GFF by some constant shift. The cosmological constant term can likewise be discarded if we measure energies relative to it. However, the quadratic term is a new counter-term interaction, whose coupling is related to the difference in normal-ordering constants, which is a well-defined quantity given by the Abel-Plana formula [30]. This quadratic counter-term is incidentally not worrisome at all. In fact, we shall be using it to tune the conformal fixed point as discussed in section 4.4. Let's now turn to building our Hamiltonian and Fock space via radial quantization.

4.2 Radial quantization and the state-operator correspondence

Suppose a CFT is defined in d-dimensional flat space endowed with the metric

$$ds^2 = dr^2 + r^2 d\Omega_{d-1}^2. (4.11)$$

Now consider the change of radial coordinate $r = e^{\tau}$. This is a conformal transformation leading to

$$ds^{2} = e^{2r} \left(d\tau^{2} + d\Omega_{d-1}^{2} \right) , \qquad (4.12)$$

which is conformal to a cylinder $\mathbb{R} \times S^{d-1}$. The real coordinate τ plays the role of time, and it can be associated with a generator of "time" translations. Recall the following relations from the conformal algebra in Euclidean signature:

$$[D, P_{\mu}] = P_{\mu}, \quad [D, K_{\mu}] = -K_{\mu},$$
 (4.13)

where P_{μ} is the generator of translations and K_{μ} that of special conformal transformations. These motivate the following identification: D can be viewed as a Hamiltonian generating time translations, while P_{μ} and K_{μ} as raising and lowering operators respectively. Viewing the theory on the cylinder as a quantum theory with τ as a direction of time is the first step towards radial quantization. Now let $\mathcal{O}(0)$ be a primary operator inserted at the origin of \mathbb{R}^d . Recall that under a conformal transformation $x \mapsto x'$, we have:

$$\mathcal{O}'(x') = \left| \frac{\partial x}{\partial x'} \right|^{\frac{\Delta}{d}} \mathcal{O}(x), \qquad (4.14)$$

which translates to the following via the sphere-cylinder map described above:

$$\mathcal{O}'(\tau) = |x|^{\Delta/d} \mathcal{O}(x). \tag{4.15}$$

Suppose that we have a Hilbert space on the cylinder on which the cylinder operators act, endowed with a conformally invariant vacuum state $|0\rangle$. We can then associate to the operator inserted at the origin of \mathbb{R}^d the state $|\mathcal{O}\rangle = \mathcal{O}'(-\infty)|0\rangle$, and subsequently time evolve this state using exponentiation of the cylinder Hamiltonian D. Note that we can obtain eigenstates of D on the cylinder using primaries at the origin:

$$D\mathcal{O}(0) \cdot |0\rangle = [D, \mathcal{O}(0)] \cdot |0\rangle = \Delta |0\rangle, \tag{4.16}$$

and descendant operators will similarly yield descendant states.

Conversely, let $|\psi(t)\rangle$ be some state on the cylinder at some fixed time slice. The state can be propagated backwards in time until it corresponds to a small sphere around the origin in \mathbb{R}^d . Using rotations, this completely fixes how the operator we wish to construct behaves on this sphere. Hence, we are left with a boundary condition which fully constrains the operator $\mathcal{O}(0)$ we are after (this can be viewed as a consequence of scale invariance) [67]. This is the famous state-operator correspondence in CFT, which allows us to interchangeably refer to operators \mathcal{O} and states $|\mathcal{O}\rangle$

4.3 Radial quantization of the generalized free field

The plane-cylinder map for a cylinder of unit radius we defined in the previous subsection leads to the following primary transformation rule in one dimension:

$$\phi_{\text{cyl}}(\tau) = |x|^{\Delta_{\phi}} \phi(x). \tag{4.17}$$

Let's now address the quantization of the GFF ϕ . While canonical quantization doesn't seem to apply here, since the kinetic term in the non-local action does not contain any time derivatives and hence there is no canonical notion of momentum, we can still proceed with the conformal field-theoretic framework of radial quantization. In this paradigm, a Hilbert space is constructed on the cylinder, consisting of a vacuum $|0\rangle$ and spanned by states obtained by acting on it with a local operator inserted at the origin of the plane in the plane-cylinder map. The free theory on the cylinder is governed by a Hamiltonian H_0 which is given by the dilation operator D assumed to be Hermitian and thus diagonalizable. Since we take this CFT to be free, it is quadratic in the GFF ϕ , and hence we expect it to be written using a sum of number operators obtained using ladder operators:

$$H_0 = D = \sum_{n=0}^{\infty} (\Delta + n) a_n^{\dagger} a_n , \qquad (4.18)$$

where $[a_n, a_m^{\dagger}] = \delta_{mn}$. Note that in the Heisenberg picture in Euclidean signature

$$\frac{d}{d\tau}a_n = [H_0, a_n] = -(\Delta + n)a_n,$$

$$\frac{d}{d\tau}a_n^{\dagger} = [H_0, a_n^{\dagger}] = (\Delta + n)a_n^{\dagger},$$
(4.19)

and thus one sensible ansatz for the field operators acting on the cylinder Hilbert space is

$$\phi_R(\tau) = \sum_{n=0}^{\infty} \frac{1}{r_n} \left[e^{-(\Delta_{\phi} + n)\tau} a_n + e^{(\Delta_{\phi} + n)\tau} a_n^{\dagger} \right] ,$$

$$\phi_L(\tau) = \sum_{n=0}^{\infty} \frac{1}{l_n} \left[e^{-(\Delta_{\phi} + n)\tau} a_n + e^{(\Delta_{\phi} + n)\tau} a_n^{\dagger} \right] ,$$

$$(4.20)$$

where l_n, r_n are left and right normalizations to be fixed later. The plane-cylinder map coupled to the primary operator transformation rule tell us that

$$\phi(x > 0) = \sum_{n=0}^{\infty} \frac{1}{r_n} \left[|x|^{-2\Delta_{\phi}} x^{-n} a_n + x^n a_n^{\dagger} \right] ,$$

$$\phi(x < 0) = \sum_{n=0}^{\infty} (-1)^n \frac{1}{l_n} \left[|x|^{-2\Delta_{\phi}} x^{-n} a_n + x^n a_n^{\dagger} \right] .$$
(4.21)

Requiring that ϕ be continuous at the origin leads to $l_n = (-1)^n r_n$ and

$$\phi(x) = \sum_{n=0}^{\infty} \frac{1}{r_n} \left[\frac{a_n}{|x|^{2\Delta}} x^{-n} + a_n^{\dagger} x^n \right]. \tag{4.22}$$

Lastly, in order to fix the value of r_n , we require that $\langle 0|\phi(x)\phi(y)|0\rangle = |x-y|^{-2\Delta_{\phi}}$ in accordance with the behavior of a GFF in CFT. Indeed, for |x| > |y|:

$$\langle 0|\phi(x)\phi(y)|0\rangle = \frac{1}{|x|^{2\Delta}} \sum_{n=0}^{\infty} r_n^{-2} \frac{y^n}{x^n} = \frac{1}{|x|^{2\Delta}} \frac{1}{(1-y/x)^{2\Delta}} = \frac{1}{|x-y|^{2\Delta}}$$
(4.23)

provided that

$$r_n^{-2} = \frac{(2\Delta_\phi)_n}{n!} \,, \tag{4.24}$$

where we define the Pochhammer symbol by $(x)_y = x(x+1) \dots (x+y-1)$. Our cylinder operators then take their final form

$$\phi_R(\tau) = \sum_{n=0}^{\infty} \sqrt{\frac{(2\Delta_{\phi})_n}{n!}} \left[e^{-(\Delta_{\phi} + n)\tau} a_n + e^{(\Delta_{\phi} + n)\tau} a_n^{\dagger} \right],$$

$$\phi_L(\tau) = \sum_{n=0}^{\infty} (-1)^n \sqrt{\frac{(2\Delta_{\phi})_n}{n!}} \left[e^{-(\Delta_{\phi} + n)\tau} a_n + e^{(\Delta_{\phi} + n)\tau} a_n^{\dagger} \right].$$

$$(4.25)$$

Next, we should build an orthonormal basis for our Fock space

$$\mathcal{F} = \mathcal{H} \oplus \mathcal{H}^{\otimes 2} \oplus \mathcal{H}^{\otimes 3} \oplus \dots \tag{4.26}$$

where \mathcal{H} is a Hilbert space spanned by a vacuum state $|0\rangle$ and $a_n^{\dagger}|0\rangle$ for $n \in \mathbb{N}$. As for \mathcal{F} , it is spanned by $(a_{n_1}^{\dagger})^{k_1} \dots (a_{n_l}^{\dagger})^{k_l}|0\rangle$ for any string $(n_1, \dots, n_l), (k_1, \dots, k_l)$. These states are clearly orthogonal to each other thanks to the commutation relations of ladder operators. As for their normalization, note that $\langle 0|0\rangle = 1$ and

$$\langle 0|(a_n)^k (a_n^{\dagger})^k |0\rangle = k! \tag{4.27}$$

which entails that the following is a good orthonormal basis state:

$$|\vec{k}\rangle = \prod_{i=0}^{\infty} \frac{1}{\sqrt{k_i!}} (a_{n_i}^{\dagger})^{k_i} |0\rangle. \tag{4.28}$$

Such states are indeed unit normalized and orthogonal for different \vec{k} strings. Incidentally, these states are in one to one correspondence with the states obtained by acting with products of ϕ and its derivatives in equation (4.3), since $a_n^{\dagger}|0\rangle \propto \partial^n \phi(0)|0\rangle$. Since we'll be considering normal-ordered monomials in ϕ as our interactions, it's worth addressing the general expression for ϕ^n interactions, as well as their matrix elements. Taking normal-ordered powers of (4.25) leads to

$$: \phi_L^n(0) + \phi_R^n(0) := 2 \sum_{l_1 + \dots + l_n \in 2\mathbb{N}} \binom{n}{k} \sqrt{\frac{(2\Delta_\phi)_{l_1}}{l_1!} \dots \frac{(2\Delta_\phi)_{l_n}}{l_n!}} a_{l_1}^{\dagger} \dots a_{l_k}^{\dagger} a_{l_{k+1}} \dots a_{l_n}. \tag{4.29}$$

The condition that admissible mode indices sum to an even number enforces symmetry under space parity, i.e. even states are sent to even states and odd states are sent to odd ones by acting with ϕ^n , with parity being defined by

$$P|\vec{k}\rangle = \frac{1}{2} \left(1 + (-1)^{\sum_r r k_r} \right) |\vec{k}\rangle,$$
 (4.30)

where P should not be confused with the momentum operator here. Matrix elements of this interaction will involve factors of \sqrt{k} and $\sqrt{k+1}$ for k an occupation number. Indeed, for some mode l, $a_l^{\dagger} | \dots k_l \dots \rangle = \sqrt{k_l+1} | \dots k_l+1 \dots \rangle$, and $a_l | \dots k_l \dots \rangle = \sqrt{k_l} | \dots k_l-1 \dots \rangle$. Thus, instead of reasoning with modes, it is convenient to reason in terms of occupation numbers. This leads to the following compact expression:

$$\langle \vec{k'}|: \phi_L^n(0) + \phi_R^n(0): |\vec{k}\rangle = 2n! \sum_{\substack{\sum_r (m_r + s_r) = n \\ \sum_r r(m_r + s_r) \in 2\mathbb{N}}} \delta_{\vec{k'}, \vec{k} - \vec{m} + \vec{s}} \prod_r \frac{1}{m_r! s_r!} \sqrt{\left[\frac{(2\Delta_{\phi})_r}{r!}\right]^{s_r + m_r}} (k_r - m_r + 1)_{m_r} (k_r - m_r + 1)_{s_r},$$

$$(4.31)$$

where the additional Pochhammer symbols stem from the action of ladder operators and the factorials come from permutations of creation or annihilation operators among themselves. This is admittedly involved, yet it will prove very useful for deriving results in Rayleigh-Schrödinger perturbation theory in section 4.5. As for our numerical simulations, we'll stick with expression (4.29).

4.4 Tuning to LORI and LORALY

So far, we've been considering generic Hamiltonians with cubic or quartic interactions and arbitrary couplings. Since LORI and LORALY are by definition conformal fixed points, starting from a non-local theory with cubic or quartic interaction, we need to tune our couplings to reach a conformal fixed point. Under RG flow, we a priori need to activate all relevant interactions, hence let's briefly examine what those might be in LORI and LORALY. For LORI, ϕ , ϕ^2 and ϕ^3 are all relevant a priori. However, ϕ and ϕ^3 break \mathbb{Z}_2 symmetry and should be discarded. Hence, the full Hamiltonian for LORI should be

$$H_{\text{LORI}} = H_{CFT} + \frac{\lambda}{4!} (: \phi_L(0)^4 + \phi_R(0)^4 :) + g_2(: \phi_L(0)^2 + \phi_R(0)^2 :) + \Lambda_4 \mathbb{1},$$
(4.32)

to which we've added a cosmological constant term which shifts the vacuum scaling dimension to 0. As for LORALY, \mathbb{Z}_2 symmetry isn't present even in the underlying model. We can therefore add ϕ and ϕ^2 . However, adding a ϕ interaction amounts to shifting the VEV of the GFF, which we take to be zero anyway. As for LORI, the only relevant interaction we keep is therefore ϕ^2 , and we arrive at

$$H_{\text{LORALY}} = H_{CFT} + \frac{ig}{3!} : \phi_L(0)^3 + \phi_R(0)^3 : +g_2 : \phi_L(0)^2 + \phi_R(0)^2 : +\Lambda_3 \mathbb{1}.$$
(4.33)

Hence, we have two non-trivial couplings to tune, and therefore we ought to find the two corresponding constraints to satisfy. Since we're looking for a non-trivial interacting fixed point, a natural choice is the equation of motion. Indeed, in the equation of motion $\mathcal{L}_{\sigma}\phi \sim \phi^{n-1}$, the scaling dimensions on the LHS and RHS should match, hence the definition of the fractional Laplacian (2.23) leads to $\sigma + \Delta_{\phi} = \Delta_{\phi^{n-1}}$, which gives $\Delta_{\phi^{n-1}} = 1 - \Delta_{\phi}$ for n = 3 or 4. The next constraint comes from considering the action of the derivative on primary operators, which produces descendants. The simplest case is $\partial \phi$, whose dimension must be $\Delta_{\partial \phi} = 1 + \Delta_{\phi}$. Hence, the full constraints to satisfy are

$$\begin{cases}
\Delta_0 = 0 \\
\Delta_{\phi^3} = 1 - \Delta_{\phi} & \text{(for LORI)} \\
\Delta_{\phi^2} = 1 - \Delta_{\phi} & \text{(for LORALY)} \\
\Delta_{\partial \phi} = \Delta_{\phi} + 1
\end{cases}$$
(4.34)

Again, we can easily impose a zero-energy vacuum using a cosmological constant, but this essentially amounts to measuring energies relative to the potentially non-zero vacuum dimension Hamiltonian truncation leads to. It's worth mentioning that the Hamiltonians with tuned counter-terms above justify why, in practice, we do not worry about the discrepancy between normal-ordering on the cylinder and normal-ordering on the plane as we did at the end of section 4.1.

4.5 Comparison with Rayleigh-Schrödinger perturbation theory

While the end goal of Hamiltonian truncation is the derivation of strong coupling results, comparing truncation results for weak coupling to those derived using perturbation theory is a healthy sanity check, and it is largely to this end that we carefully derived results in the ε -expansion for LORI and LORALY in sections 3.2 and 3.3 respectively. However, as in ordinary quantum mechanics, we have other perturbative methods at our disposal, among which is Rayleigh-Schrödinger perturbation theory. The setup is the same as before, starting from $H = H_0 + V$, except we now treat V as a small perturbation. Examining the time-independent Schrödinger equation order by order in perturbation theory, we arrive at n-th order corrections to the energy eigenvalues and the corresponding eigenvectors. For a non-degenerate state $|\vec{k}\rangle$:

$$\Delta_{\vec{k}} = \Delta_{\vec{k}}^{(0)} + \langle \vec{k} | V | \vec{k} \rangle + \sum_{|\vec{l}\rangle \neq |\vec{k}\rangle} \frac{\langle \vec{k} | V | \vec{l} \rangle \langle \vec{l} | V | \vec{k} \rangle}{\Delta_{\vec{k}} - \Delta_{\vec{l}}} + O(V^3). \tag{4.35}$$

Since the first order correction depends only on the diagonal matrix element corresponding to a given operator, and not on all states up to some scaling dimension cutoff, it is not particularly sensitive to the cutoff Δ_T provided $\Delta_{\vec{k}} \leq \Delta_T$. Hence it suffices to take Δ_T equal to the UV dimension of the operator in question to determine first order corrections. Higher order corrections however are much more sensitive to the UV cutoff. It bears mentioning that the degenerate case is not that different from this case, up to an additional step of identifying degenerate subspaces and diagonalizing the restriction of V to those subspaces 6 .

In the case of LORI in one dimension, Rayleigh-Schrödinger perturbation theory is very powerful. Indeed, we've previously derived an expression for all matrix elements (4.31) of the perturbation $V \propto \phi^n$, and for even n we can have $\langle \vec{l} | \phi^n | \vec{k} \rangle \neq 0$. Using these interaction matrix elements, we easily derive the leading order correction to all operators in $g_{2n}\phi^{2n}/(2n)!$ theory – since this is low-hanging fruit – and subsequently specialize to LORI with n=2.

⁶In fact, the free Hamiltonian is no longer degenerate when working away from the value of Δ_{ϕ} at $\varepsilon = 0$.

⁷It is probably worthwhile to study a non-local theory with, say, ϕ^6 interactions at some point to test these results. We defer this to future work.

$$\Delta_{\vec{k}} = \Delta_{\vec{k}}^{(0)} + 2g_{2n} \sum_{\substack{\sum m_r = n \\ m_r \le k_n}} \prod_r \frac{1}{m_r!^2} \left[\frac{(2\Delta_{\phi})_r}{r!} \right]^{m_r} (k_r - m_r + 1)_{m_r} + O(g_{2n}^2).$$
(4.36)

In particular, this computation yields a simple, closed-form expression for the dimensions of all $(\partial^l \phi)^{k}$'s:

$$\Delta_{k,l} = k \left(\Delta_{\phi} + l \right) + \frac{2g_{2n}}{n!^2} \left[\frac{(2\Delta_{\phi})_l}{l!} \right]^2 \frac{k!}{(k-n)!} + O(g_{2n}^2), \tag{4.37}$$

from which we also derive the dimensions relevant to the conformal constraints from section 4.4:

$$\Delta_{|0\rangle} = O(g_{2n}^2), \tag{4.38}$$

$$\Delta_{\phi} = \frac{1}{2n} - \frac{\varepsilon}{2n} + O(g_{2n}^2), \qquad (4.39)$$

$$\Delta_{\phi^{2n-1}} = \frac{2n-1}{2n} (1-\varepsilon) + \frac{2g_{2n}}{n!^2} \frac{(2n-1)!}{(n-1)!} + O(g_{2n}^2), \tag{4.40}$$

$$\Delta_{\partial\phi} = \frac{1-\varepsilon}{2n} + 1 + O(g_{2n}^2). \tag{4.41}$$

Hence, we recover the fact that ϕ does not acquire an anomalous dimension at least at one loop order (we know this holds exactly of course). Imposing $\Delta_{\phi^{2n-1}} = 1 - \Delta_{\phi}$ as per the conformality constraints leads to ⁸

$$g_{2n}^* = \frac{n!^2(n-1)!}{2(2n-1)!}\varepsilon + O(\varepsilon^2), \qquad (4.42)$$

and n=2 is consistent with the known result for LORI, namely $\lambda_* = \varepsilon/3 + O(\varepsilon^2)$, derived previously using Feynman diagrams. A priori, this did not have to be the case, since the coupling is not a physical observable and is scheme dependent. This can be related to the fact that the first order correction turns out to be scheme independent, which is not the case a priori for second order corrections. For LORALY, we'll notice a deviation at lowest non-trivial order, that order being 2. Incidentally, the constraint on descendants does not yield additional information on the fixed point at first order. Hence there is no need to introduce all possible \mathbb{Z}_2 and parity-symmetric counter-terms less relevant than ϕ^{2n} to leading order in perturbation theory, and all of the corresponding couplings would therefore be at most of order $O(\varepsilon^2)$. We can now specialize some of the results of this subsection to the fixed point. For example, the scaling of $(\partial^l \phi)^k$ in ϕ^{2n} theory is

$$\Delta_{k,l} = k \left(\frac{1}{2n} + l \right) + \left[\frac{k! \Gamma \left(l + \frac{1}{n} \right)^2 (n-1)!}{l!^2 (k-n)! \Gamma \left(\frac{1}{n} \right)^2 (2n-1)!} - \frac{k}{2n} \right] \varepsilon + O(\varepsilon^2),$$
(4.43)

which reproduces the known result derived in the ε -expansion of LORI for the anomalous dimension of ϕ^m for n=2, l=0 [56]: $\gamma_{\phi^n}=k(k-1)\varepsilon/6+O(\varepsilon^2)$. Quite remarkably, the previous analysis gives us the scaling dimensions of all operators in ϕ^{2n} theory to leading order in perturbation theory (up to a non-trivial sum):

$$\Delta_{\vec{k}} = \Delta_{\vec{k}}^{(0)} + \frac{n!^2(n-1)!}{(2n-1)!} \varepsilon \sum_{\substack{\sum m_r = n \\ m_r < k_r}} \prod_r \frac{1}{m_r!^2} \left[\frac{(2\Delta_{\phi})_r}{r!} \right]^{m_r} (k_r - m_r + 1)_{m_r} + O(\varepsilon^2).$$
(4.44)

In order to obtain the $O(\varepsilon^2)$ corrections, including counter-term interactions, we would need to go to second order in g_{2n} . However, the combinatorics rapidly become intricate, and this method becomes impractical for analytical study. Unfortunately, in the case of LORALY, cubic interactions cannot stabilize a given state, therefore first order corrections all vanish and the leading order contribution is $O(g^2)^{-9}$. Hence one cannot as easily derive general perturbative statements about ϕ^{2n+1} theory.

4.6 Numerical workflow and results

We now describe in detail the Hamiltonian truncation procedure used to compute spectra in LORI and LORALY. The implementation is centered around a symbolic and sparse representation of the truncated Hamiltonian, built in a GFF Fock basis. The entire workflow is handled in Python using sympy for symbolic algebra, numpy and scipy.sparse for matrix representations and eigenvalue solvers, and joblib for parallel processing.

⁸Incidentally, these considerations suggest a large n analysis could lead to some interesting insights. We leave this for further work.

⁹This is consistent with $g_* \sim \sqrt{\varepsilon}$

Construction of the Fock Space The Hilbert space is constructed as the Fock space of a GFF ϕ with scaling dimension Δ_{ϕ} , as described in section 4.3. A Fock state is characterized by a vector $\vec{k} = (k_0, k_1, \dots, k_N)$ for and $N = \lfloor \Delta_T \rfloor$. To efficiently enumerate these states, our algorithm loops over the total number of field insertions $n = 0, 1, \dots, \lfloor \Delta_T / \Delta_{\phi} \rfloor$, and for each fixed number, generates all integer partitions of n into N non-negative integers, each partition corresponding to an n-particle state. The scaling dimension of the state is then given by

$$\Delta_{\vec{k}} = \sum_{i=0}^{N} k_i (\Delta_{\phi} + i).$$

By construction, only states for which $\Delta_{\vec{k}} \leq \Delta_T$ are retained. Furthermore, LORI and LORALY have additional symmetries, both being invariant under space parity and the former under $\mathbb{Z}_2: \phi \to -\phi$. Hence we also compute the corresponding quantum numbers and classify states in even or odd sectors for up to two symmetries when they exist:

$$P_{\vec{k}} = \sum_{r} r k_r \mod 2, \quad S_{\vec{k}} = \sum_{r} k_r \mod 2.$$
 (4.45)

This symmetry decomposition is essential, as it allows the Hamiltonian to be block-diagonalized, thereby considerably simplifying numerical diagonalization. Moreover, this also helps distinguish states which otherwise have dimensions very close to each other, such as ϕ^5 and $\partial \phi$ in LORI or ϕ^4 and $\partial \phi$ in LORALY. This step is one of the main bottlenecks of our code, and as such it is convenient to build a very large Fock space once and for all, which we subsequently reuse and re-truncate to smaller Δ_T to our convenience.

Construction of the free Hamiltonian The free Hamiltonian is constructed directly from the scaling dimensions of the basis states. This matrix is diagonal, and is constructed symbolically using sympy. The entries depend only on the symbolic variable Δ_{ϕ} , which is left unevaluated during matrix construction. This allows the same symbolic matrix to be reused for different values of Δ_{ϕ} during parameter sweeps or fixed point tuning.

Construction of the interaction Hamiltonian To construct the matrix representation of ϕ^n within a given symmetry sector, the algorithm proceeds column by column, leveraging expression (4.29). For each state in the sector – corresponding to a column – it evaluates the action of : ϕ^n : by iterating over all admissible n-tuples of modes (l_1, \ldots, l_n) satisfying the constraint $\sum_r l_r \in 2\mathbb{N}$, which ensures parity conservation. For each such tuple, the algorithm generates all normal-ordered assignments of creation and annihilation operators across the modes. It subsequently applies the product of ladder operators resulting from a given assignment to the state. If the output state has a scaling dimension below the cutoff, it contributes a non-zero coefficient to the associated line in the aforementioned column. Because each column each matrix element can be computed independently, the matrix assembly is parallelized using joblib.Parallel. The space of columns is divided into batches and evaluated concurrently across CPU cores¹⁰.

This logic is implemented symbolically, with all matrix entries computed as exact expressions in Δ_{ϕ} once and for all for a maximal truncation Δ_{T} . The prefactors are derived from multinomial combinatorics and are simplified using symbolic factorials and Γ -functions. To avoid excessive memory usage, the interaction matrix is stored in SparseMatrix format from the sympy module, recording only non-zero triplets (i, j, value) as symbolic expressions. For efficient symbol substitution, we then use sympy.lambdify to generate compiled functions of the numerical value of Δ_{ϕ} which return scipy.sparse CSR matrices for each interaction.

Diagonalization, spectrum extraction and tuning The Hamiltonians for each sector are assembled for a given set of coupling as weighted sums of the arrays computed in the previous step. They can be diagonalized using scipy.sparse.linalg.eigs for LORALY (non Hermitian), and the spectra are shifted so as to have a zero-energy ground state, i.e. the lowest parity and \mathbb{Z}_2 -even state. To enforce conformal invariance at a given $\Delta_{\phi} = (1 - \varepsilon)/3$ or $(1 - \varepsilon)/4$, we first read out the physical scaling of ϕ , say $\Delta_{\phi}^{(1)}$ (which is in general distinct from the parameter Δ_{ϕ}), and then define a cost function F which computes the residuals

$$F(g_2, g_n) = \begin{cases} \Delta_{\phi^{n-1}} - \left(1 - \Delta_{\phi}^{(1)}\right) & (n = 4 \text{ or } 3 \text{ for LORI/LORALY}) \\ \Delta_{\partial \phi} - \left(1 + \Delta_{\phi}^{(1)}\right) & \end{cases}$$
(4.46)

 $^{^{10}}$ This was conducted on a laptop with eight CPU cores. This workflow will eventually be replicated on a computer cluster to reach higher truncations Δ_T and compute Fock states and matrix elements faster.

with $\Delta_{\phi^{n-1}}$ taken to be in the parity-even sector of the spectrum, and perhaps \mathbb{Z}_2 -odd when we're studying LORI, and $\Delta_{\partial\phi}$ is taken to be in the parity-odd, and \mathbb{Z}_2 -odd sector for LORI. We use a root finding function scipy.optimize.root, which adjusts the counter-term coefficients g_i until $F(g_1, g_{n+1}) \approx 0$, typically up to an error between 10^{-15} and 10^{-10} . Typically, convergence is achieved rapidly with good numerical stability, although a good initial guess for root finding at a given iteration is often the value of the optimal couplings from the previous iteration.

Parameter Sweeps and Results To study the RG flow and fixed point behavior, the full numerical pipeline is executed over a grid of UV parameters: $0 \le \varepsilon \le \varepsilon_{\text{max}}$ with $\varepsilon_{\text{max}} = 0.01$ in the plots below, such that $\Delta_{\phi} = (1-\varepsilon)/4$ or $(1-\varepsilon)/3$; truncation levels $0 \le \Delta_T \le 10$. For each (ε, Δ_T) pair: the zero of the cost function $F(g_2, g_n)$ is determined and the zero and resulting spectrum are stored for plotting. These results are compared against the ε -expansion results from sections 3.2 and 3.3. To plot physical quantities, we first extract an effective ε related to the physical $\Delta_{\phi}^{(1)}$ extracted from the spectrum:

$$\varepsilon_{\text{eff}} = 1 - 4\Delta_{\phi}^{(1)} \text{ (LORI) or } 1 - 3\Delta_{\phi}^{(1)} \text{ (LORALY)}.$$
 (4.47)

In each case, the agreement is excellent at small ε_{eff} , and systematic deviations at larger ε reflect the influence of higher-order corrections and truncation effects (see figures 1, 2 and 3).

5 Effective Hamiltonians and renormalization

5.1 Next-to-leading order effective Hamiltonian

So far, we've been assuming that

$$\forall |i\rangle, |f\rangle \in \mathcal{H}_{\text{eff}}, \langle f|H_{\text{eff}}|i\rangle \approx \langle f|H|i\rangle,$$
 (5.1)

and previous numerical results suggest that this is not too far off. However, increasing the cutoff Δ_T past Δ_T of the order of 10 (on a laptop using local parallelization) is difficult, and the optimization algorithm does not always converge as we increase ε past $\varepsilon = 0.1$. This suggests that the truncated Hamiltonian we've been working with was too naive. Indeed, if we adopt the Wilsonian picture involving integrating out high energy modes, then what we've done amounts to merely forgetting those high energy modes, instead of writing a theory for the low energy states incorporating the effect of the high energy ones. Therefore, let's be more systematic about integrating out the high energy states, and construct a more faithful effective Hamiltonian. To do so, we will match an observable in the fundamental theory described by $H = H_0 + V$ to its equivalent in an effective theory described by

$$H_{\text{eff}} = H_0 + H_1 + H_2 + \dots,$$
 (5.2)

where $H_k = O(V^k)$. The observable we'll be matching is the transition matrix, which we will work towards defining now, essentially reproducing the reasoning in [50]. For starters, suppose we adiabatically turn off the V interactions at some rate ϵ :

$$H = H_0 + Ve^{-\epsilon t} \,. \tag{5.3}$$

The role ϵ plays will become clear shortly. Next, take an initial state $|i\rangle$, and time evolve it to $|f\rangle$ using H on the one hand, and the currently undetermined H_{eff} on the other. We would like to have

$$\langle f|e^{-iH_{\text{eff}}t_f}|i\rangle = \langle f|T\exp\left(-i\int_0^\infty dt(H_0 + Ve^{-\epsilon t})\right)|i\rangle,$$
 (5.4)

however this cannot be quite right since in the eigenbasis of H_0 we have an undefined phase on the LHS as $t_f \to \infty$. This subtlety can be taken care of by going to the interaction picture:

$$|\psi(t)\rangle_I := e^{iH_0 t} |\psi(t)\rangle_S, \quad \mathcal{O}_I(t) := e^{iH_0 t} \mathcal{O}_S e^{-iH_0 t},$$
 (5.5)

where the subscript S indicates the quantity in the Schrödinger picture, and I indicates the corresponding quantity in the interaction picture. Defining $V_I(t) = e^{iH_0t}Ve^{-\epsilon t}e^{-iH_0t}$, the interaction picture time evolution operator is given by a time-ordered exponential:

$$U_I(t_f, t_i) = T \exp\left(-i \int_{t_i}^{t_f} dt V_I(t)\right). \tag{5.6}$$

Indeed, the time evolution operator obeys a Schrödinger-like equation,

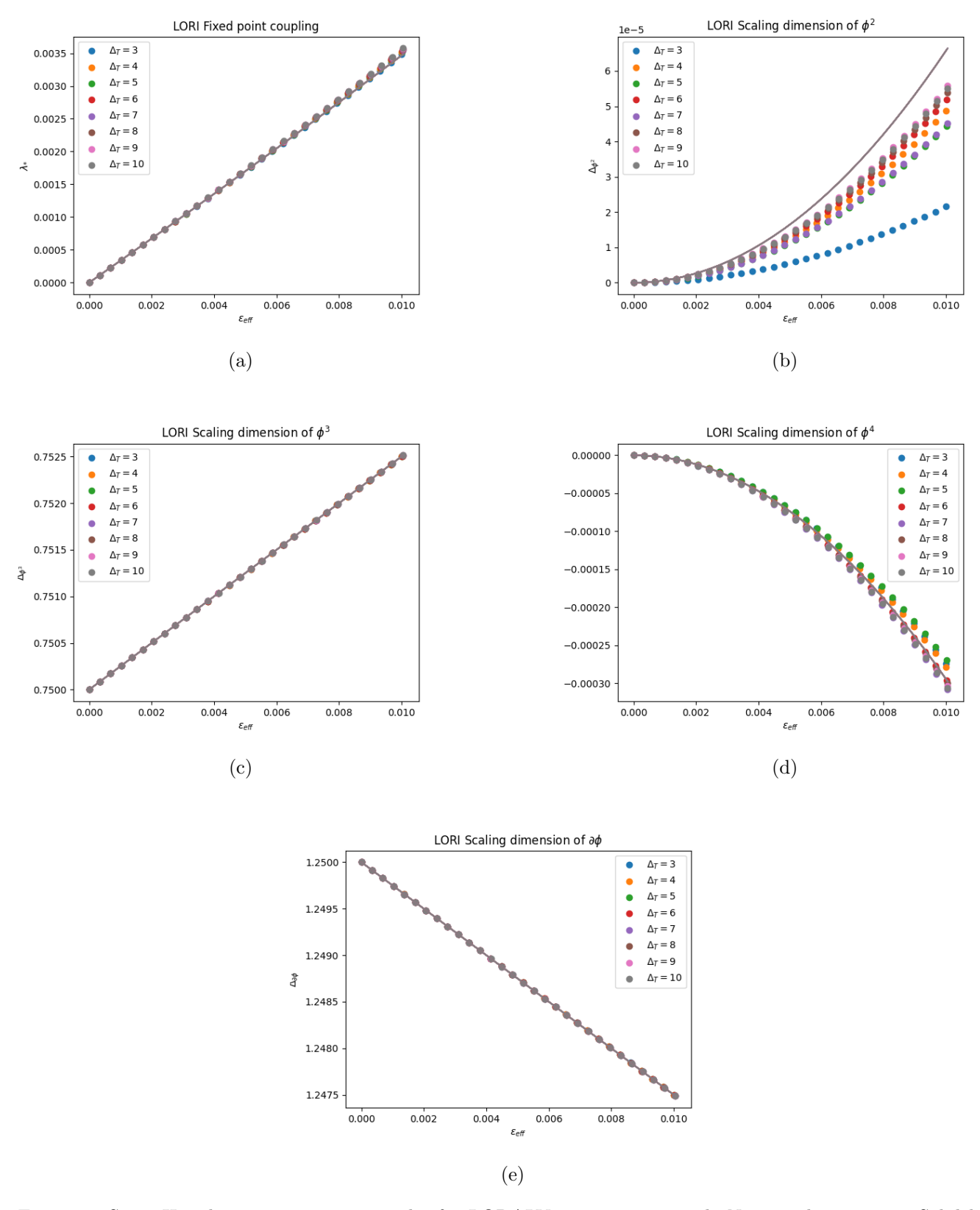


Figure 1: Some Hamiltonian truncation results for LORALY, $\varepsilon_{\text{max}} = 0.01$ with N = 30 data points. Solid lines indicate theoretical predictions, scatter plots are used for truncation results. Notice the agreement between the theoretical coupling and the tuning result in (a) to first order in ε . This is due to the fact that quantum corrections appear at first order in the coupling for LORI, and the first order renormalization constant is scheme independent. In (c) and (e) the dimensions which are involved in the tuning procedure are shown, and clearly a suitable fixed point was found for every studied value of ε . In (b) and (d), we only plot the second order correction to the scaling dimension, and for higher Δ_T there appears to be agreement with the theoretical prediction.

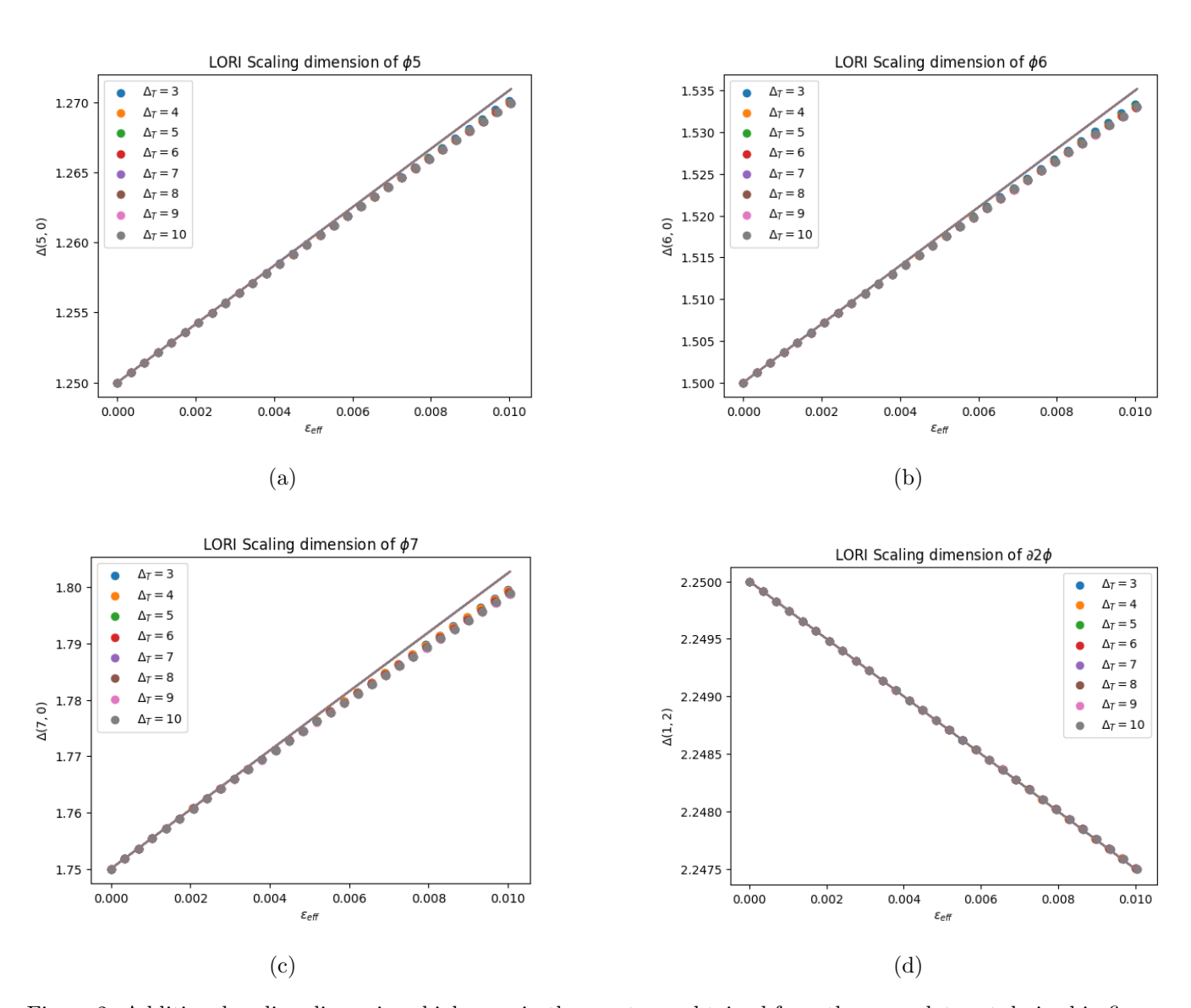


Figure 2: Additional scaling dimensions higher up in the spectrum obtained from the same data set derived in figure 1, and following the same conventions. These display excellent agreement with the general expression (4.43).

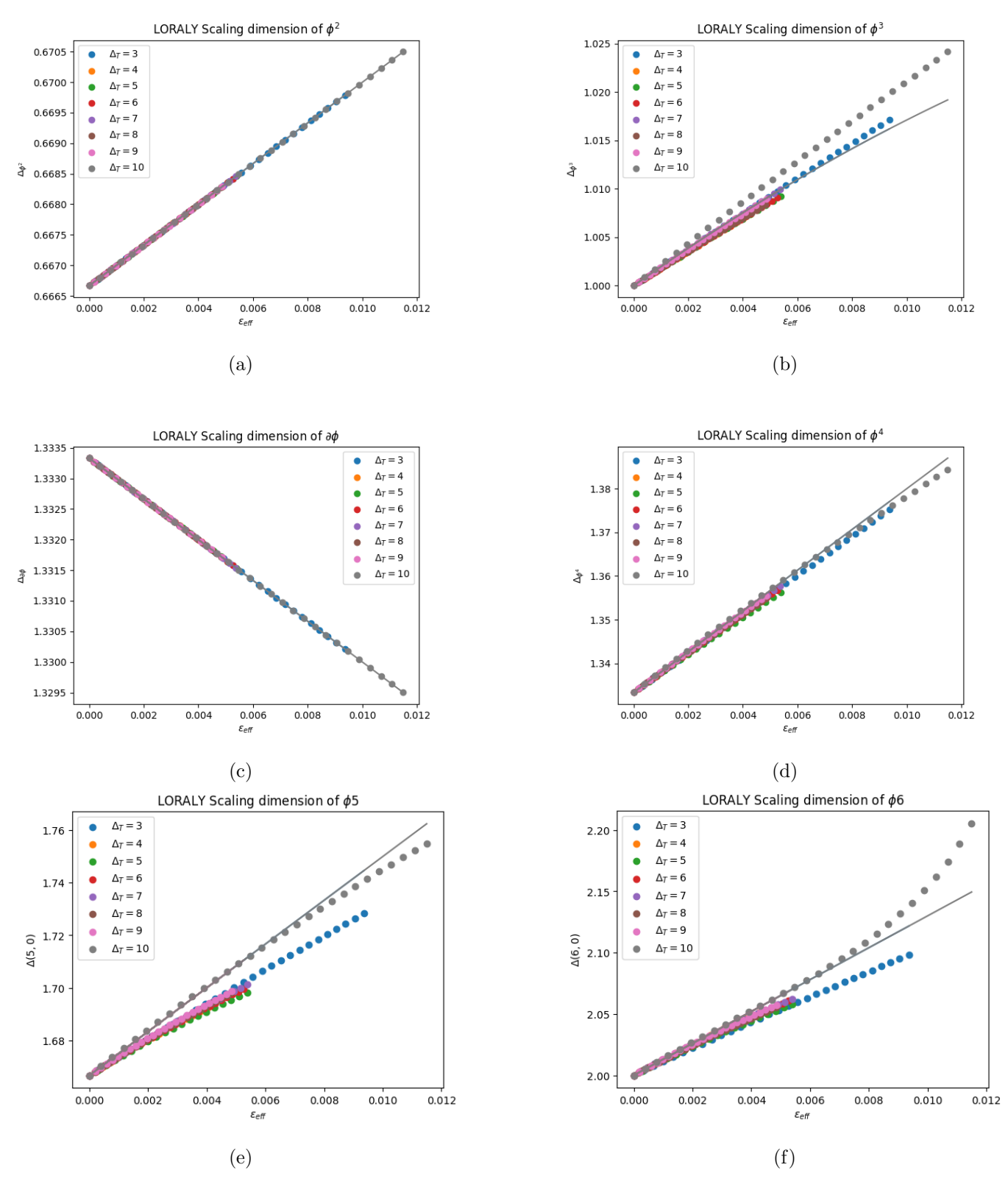


Figure 3: Some Hamiltonian truncation results for LORALY, $\varepsilon_{\text{max}} = 0.01$ with N = 30 data points. Solid lines indicate theoretical predictions, scatter plots are used for truncation results. Notice here that results are not as good as for LORI. This is due to the fact that quantum corrections only appear at second order in the coupling for LORALY, and the second order renormalization constant is scheme dependent. In short, successive corrections are much more sensitive to Δ_T . In (a) and (c) the dimensions which are involved in the tuning procedure are shown, and clearly a suitable fixed point was found for every studied value of ε . While the slopes seem to be reasonable compared to perturbation theory, the plots seem to oscillate around the correct theoretical slope; this might be attributed to the imaginary coupling of LORALY.

$$\frac{\partial}{\partial t_i} U_I(t_f, t_i) = i U_I(t_f, t_i) V_I(t_i), \quad U_I(t_f, t_f) = 1.$$

$$(5.7)$$

This is subsequently solved using a Dyson series expansion, which is formally identified as (5.6). Next, let's define an operator analogous to the S-matrix, whose matrix elements are given by

$$\langle f|\Sigma(\epsilon)|i\rangle := \lim_{t_f \to \infty} \langle f|U_I(t_f, 0)|i\rangle.$$
 (5.8)

Plugging the expression (5.6) into this definition leads to

$$\langle f|\Sigma|i\rangle = \delta_{fi} + \frac{\langle f|V|i\rangle}{\Delta_{fi} + i\epsilon} + \sum_{\alpha} \frac{\langle f|V|\alpha\rangle\langle\alpha|V|i\rangle}{(\Delta_{fi} + i\epsilon)(\Delta_{f\alpha} + i\epsilon)} + O(V^3), \qquad (5.9)$$

where from now on we also denote energy differences $\Delta_{fh} = \Delta_f - \Delta_h$. This is almost the observable we'll be matching, however a more convenient quantity is the transition matrix T, defined by

$$\langle f|\Sigma|i\rangle = \delta_{fi} + \frac{\langle f|T|i\rangle}{\Delta_{fi} + i\epsilon},$$
 (5.10)

which then reads

$$\langle f|T|i\rangle = \langle f|V|i\rangle + \sum_{\alpha} \frac{\langle f|V|\alpha\rangle\langle\alpha|V|i\rangle}{\Delta_{f\alpha} + i\epsilon} + O(V^3).$$
 (5.11)

Note that $|f\rangle$ is included in the states which are summed over, namely all of them. Hence, as $\epsilon \to 0$, the transition matrix appears to be ill-defined! As it turns out, this will not affect the effective Hamiltonian, which behaves nicely as the IR regulator ϵ vanishes. We are now fully equipped to construct an effective Hamiltonian. The expression (5.11) is valid for the Hamiltonian of the fundamental theory (5.3). The transition matrix for the effective theory (5.3) reads

$$\langle f|T|i\rangle = \langle f|H_1|i\rangle + \langle f|H_2|i\rangle + \sum_{\Delta_{\alpha} \leq \Delta_T} \frac{\langle f|H_1|\alpha\rangle\langle\alpha|H_1|i\rangle}{\Delta_{f\alpha} + i\epsilon} + O(V^3).$$
 (5.12)

Matching (5.12) and (5.11) order by order in V leads to:

$$\langle f|H_1|i\rangle = \langle f|V|i\rangle ,$$

$$\langle f|H_2|i\rangle = \sum_{\Delta_h > \Delta_T} \frac{\langle f|V|h\rangle\langle h|V|i\rangle}{\Delta_{fh} + i\epsilon} \xrightarrow[\epsilon \to 0]{} \sum_{\Delta_h > \Delta_T} \frac{\langle f|V|h\rangle\langle h|V|i\rangle}{\Delta_{fh}} .$$
(5.13)

where the upper bound on the summation symbol indicates that we are summing over states with energies greater than the UV cutoff Δ_T . There are similarly more involved expressions for $H_{k\geq 3}$ as functions of matrix elements of V and putting both low and high energy states at play (see [50, 51] for the expression of the third order correction which exemplifies this). Quite reassuringly, the effective Hamiltonian is well-defined at $\epsilon = 0$, and we can now safely drop the IR regulator. Incidentally, one might naively assume that there is a unique H_{eff} given a cutoff Δ_T . This is however not the case, since we can for example choose another scheme for perturbation theory – leveraging the Schrieffer-Wolff transformation for example – or pick other observables to match between the effective and fundamental theories. Examples of alternative prescriptions for building an effective Hamiltonian are given in [50, 51]. For the remainder of this section, we exclusively use the following expansion of the effective Hamiltonian:

$$\langle f|H_{\text{eff}}|i\rangle = \langle f|H_0|i\rangle + \langle f|V|i\rangle + \sum_{\Delta_h > \Delta_T} \frac{\langle f|V|h\rangle\langle h|V|i\rangle}{\Delta_{fh}} + \dots$$
 (5.14)

5.2 Numerical results

While, as of yet, we haven't pushed our simulations to the point that effective Hamiltonians become crucial, a simple example is enough to show that they can drastically improve results at low cutoff. Since, in practice, we cannot sum over all heavy states, we introduce an upper bound on their scaling dimensions. Let's therefore sum over all heavy states of dimension Δ such that $\Delta_T \leq \Delta \leq \Delta_T + \Delta_h$. We've implemented this strategy for LORI in figure 4, at fixed truncation $\Delta_T \in \{3, 4, 5, 6\}$. This amounted to reusing the same workflow as in section 4.6, except now with the next-to-leading order effective Hamiltonian, and looping over values of Δ_h instead of Δ_T .

Notice that, give or take some oscillation for intermediate values of Δ_h , generally speaking a maximal Δ_h improves agreement with perturbation theory, and in fact yields results comparable to maximal Δ_T . More strikingly, a lower

cutoff Δ_T and a maximal Δ_h can in fact yield more faithful results than a maximal Δ_T for the naive Hamiltonian without next-to-leading order corrections (i.e. $\Delta_h = 0$). Furthermore, there seems to be a tradeoff between Δ_T and Δ_h , given a maximal value of $\Delta_T + \Delta_h$ related to our Fock space construction. For Δ_T too small, a large Δ_h improves agreement but it is not optimal. For Δ_T too large, we are forced to work with small Δ_h , and thus next-to-leading-order corrections become negligible. However, for $\Delta_T \approx \Delta_h$, we find excellent agreement with perturbation theory, which behaves even better than maximal Δ_T ¹¹.Hence, it seems we want just enough light states to reasonably reproduce our low energy spectrum, but just enough heavy states to properly account for UV effects. This is significant, since it allows us to work with smaller Hamiltonians which are much faster to diagonalize. For example, when going from $\Delta_T = 10$ to $\Delta_T = 5$, each sector of our Hamiltonian is smaller by an order of magnitude.

5.3 UV divergences

We've recovered results in the ε -expansion for some fixed UV cutoff Δ_T and using effective Hamiltonians. To do so, we solved for couplings satisfying some conformality constraints. Presumably, one would next want to extrapolate these results to $\Delta_T \to \infty$. Recall that in the ε -expansion, the derivation of the scale dependence of couplings is intimately related to UV divergences. Let's discuss how these might appear in Hamiltonian truncation as we increase the UV cutoff to infinity.

There are many observables which are subject to UV divergences, but the simplest one is the vacuum – or Casimir – energy. The arguments presented below generalize to arbitrary observables, but this simple example adapted from [51] will suffice for our purposes. Let's briefly set the Hamiltonian approach aside and go back to the path integral, since we will obtain qualitative results which correspond to those we will also derive in the effective Hamiltonian formalism. Suppose our deforming operator is $\mathcal{O}(\tau, x)$ on the cylinder. The relevant action is

$$S = S_0 + g \int_{\mathbb{R} \times S^{d-1}} d\tau d^{d-1} x \mathcal{O}(\tau, x) . \tag{5.15}$$

The ground state energy can be found from the path integral. Indeed, recalling that the path integral can be derived from the Euclidean propagator, consider the propagator from the vacuum at time -T/2 back to the vacuum at time +T/2, T corresponding to cylindrical time:

$$Z_T := \langle 0|e^{-HT}|0\rangle = \sum_n e^{-E_n T} \langle n|0\rangle \langle n|0\rangle, \qquad (5.16)$$

where we've expanded states in the eigenbasis of the Hamiltonian H of the theory. As $T \to \infty$, only the ground state contribution remains asymptotically, and hence $Z_T \sim e^{-E_0 T}$. We therefore arrive at the following definition of the vacuum energy:

$$E_0 = -\lim_{T \to \infty} \frac{1}{T} \log Z_T. \tag{5.17}$$

 Z_T is the partition function of the finite cylinder with $\tau \in [-T/2, T/2]$. Since connected correlation functions evaluated in the free theory generate the logarithm of the partition function, we arrive at

$$E_0 = -\lim_{T \to \infty} \frac{1}{T} \sum_{n=0}^{\infty} \frac{(-g)^n}{n!} \int d\tau_1 d^{d-1} x_1 \dots d\tau_n d^{d-1} x_n \langle \mathcal{O}(\tau_1, x_1) \dots \mathcal{O}(\tau_n, x_n) \rangle_0^c.$$
 (5.18)

By time translation invariance of the correlator, the integrand only depends on time differences, hence we can integrate over τ_n for example and reduce our problem to n-1 time integrals. This incidentally gives us a factor of T eliminating the T in the denominator, and we can safely take the limit $T \to \infty$:

$$E_0 = -\sum_{n=0}^{\infty} \frac{(-g)^n}{n!} \int d\tau_1 \dots d\tau_{n-1} d^{d-1} x_1 \dots d^{d-1} x_n \langle \mathcal{O}(\tau_1, x_1) \dots \mathcal{O}(0, x_n) \rangle_0^c$$
 (5.19)

Let's go from the cylinder to the plane. Using the relevant plane-cylinder map $\tau \to |x| = e^{\tau}$ and its effect on primaries, $\mathcal{O}(\tau, \vec{x}) = |x|^{\Delta} \mathcal{O}(x)$, we arrive at:

$$E_0 = -\frac{2\pi^{\frac{d}{2}}}{\Gamma(\frac{d}{2})} \sum_{n=0}^{\infty} \frac{(-g)^n}{n!} \int \prod_{i=1}^{n-1} d^d x_i |x_i|^{\Delta - d} \langle \mathcal{O}(x_1) \dots \mathcal{O}(x_{n-1}) \mathcal{O}(1) \rangle_0^c.$$
 (5.20)

¹¹This interpretation is not bullet proof. In fact, one would still expect that increasing Δ_T yields better results. This might be attributed to the appearance of UV divergences, discussed in the next section.

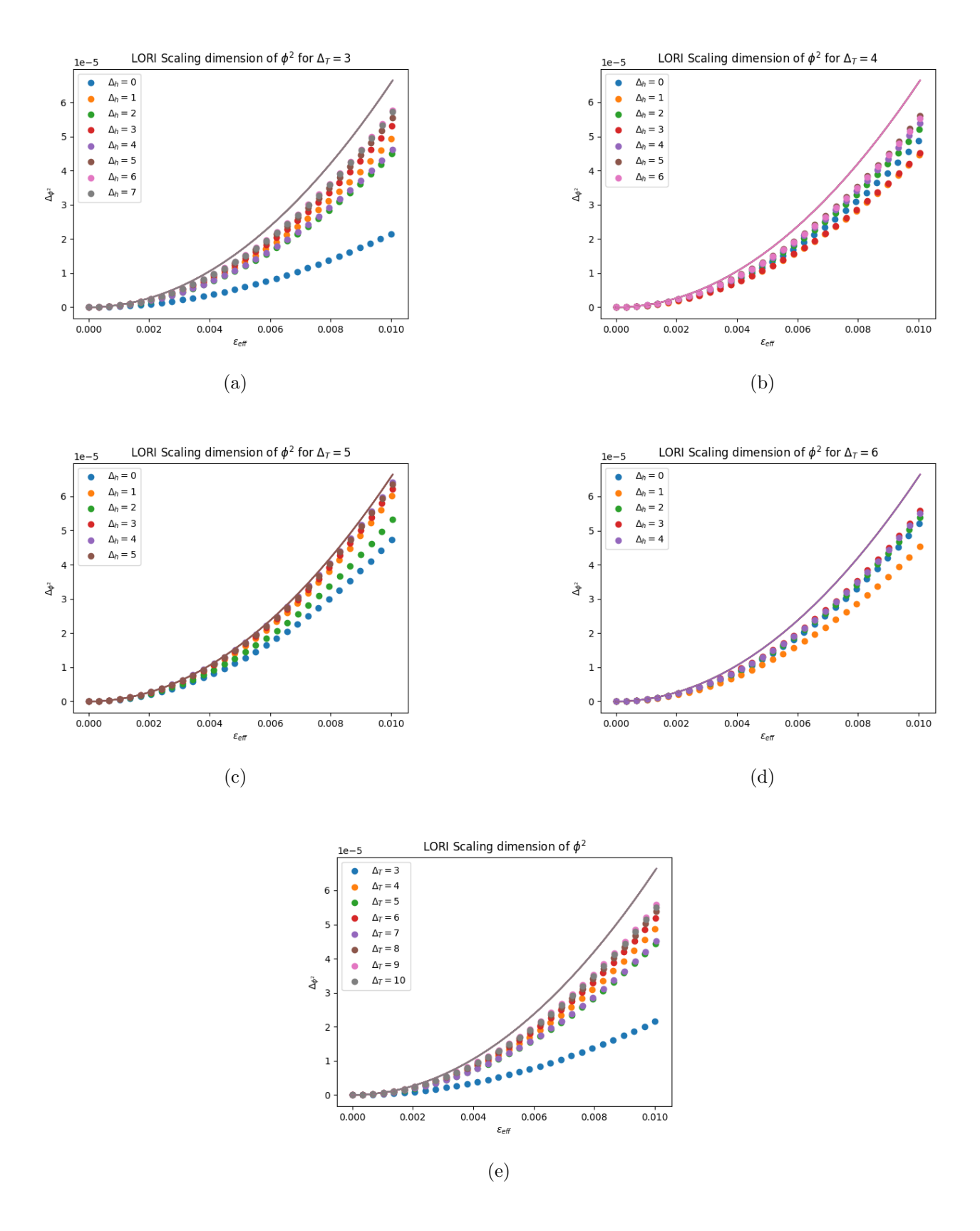


Figure 4: Same numerical setup as in figure 1. The plots in (e) are reproduced from figure 1 and included for comparison. Figures (a), (b), (d), (d) are generated using an effective Hamiltonian, including heavy states whose dimensions lie between Δ_T and $\Delta_T + \Delta_h$.

where the overall factor comes from the leftover solid angle integral stemming from the integral over the n-th coordinates with $\tau_n = 0$. Since we are not working with defects, fields can be taken to have a vanishing VEV¹². Hence the lowest order non-trivial contribution to the Casimir energy is

$$E_0^{(2)} \sim g^2 \int \frac{d^d x}{|x|^{d-\Delta}|x-1|^{2\Delta}},$$
 (5.21)

which is convergent if and only if $\Delta < d/2$. The third order contribution is

$$E_0^{(3)} \sim g^3 \int \frac{d^d x d^d y}{|x|^{d-\Delta} |y|^{d-\Delta} |x-1|^{\Delta} |y-1|^{\Delta} |x-y|^{\Delta}} \supset g^3 \int \frac{d^d x d^d y}{|x-1|^{2\Delta} |x-y|^{\Delta}} = g^3 \frac{w_{2\Delta} w_{\Delta}}{w_{3\Delta-d}} \int \frac{d^d y}{|y|^{3\Delta-d}}.$$
 (5.22)

This is convergent if and only if $\Delta < 2d/3$. This argument easily generalizes to the following statement:

$$E_0^{(n)}$$
 convergent $\Leftrightarrow \Delta < \frac{n-1}{n}d$ (5.23)

Hence as we increase Δ , more and more contributions diverge, until we hit marginality $\Delta = d$ and all n-th order corrections diverge. Such divergences generally occur for other observables as well, and one has to renormalize the theory in order to derive physical result, typically by introducing relevant counter-terms and tuning them to cancel divergences. In usual QFT, this leads to a β -function and then to a conformal fixed point. In our previous setup without the next-to-leading order corrections to the effective Hamiltonian, when tuning to LORI or LORALY, we were immediately tuning to the fixed point, thus bypassing the step where we first absorb divergences into local counter-terms. Throughout our numerical computations, we were in principle safe from this class of divergences.

How about the next-to-leading order Hamiltonian? It turns out it also has its own class of divergences, which are not cured by merely addressing the leading order case. To see this, let's turn back to radial quantization in our specific case of ϕ^n interactions. Let's study the convergence of following matrix element in the next-to-leading order effective theory¹³:

$$\langle 0|H_{\text{eff}}|0\rangle = g\langle 0|: \phi_L^n(0) + \phi_R^n(0): |0\rangle - g^2 \sum_{\Delta_T > \Delta_T} \frac{|\langle \vec{k}|: \phi_L^n(0) + \phi_R^n(0): |0\rangle|^2}{\Delta_{\vec{k}}} + O(g^3)$$
(5.24)

where again clearly: $\phi_{L,R}^n(0)$: do not stabilize the vacuum, hence the lowest non-trivial order correction is

$$\langle 0|H_{\text{eff 2}}|0\rangle = -g^2 \sum_{\Delta_{\vec{k}} > \Delta_T} \frac{|\langle \vec{k}| : \phi_L^n(0) + \phi_R^n(0) : |0\rangle|^2}{\Delta_{\vec{k}}}.$$
 (5.25)

According to equation (4.31), the only states $|\vec{k}\rangle$ that can be reached from the vacuum for this interaction are those such that $\sum_r k_r = n$ (i.e. the occupation numbers are shifted n times) and $\sum_r rk_r$ is even (i.e. conservation of parity). The relevant matrix element is then

$$\langle \vec{k} | : \phi_L^n(0) + \phi_R^n(0) : |0\rangle = 2n! \prod_r \sqrt{\frac{1}{k_r!} \left(\frac{(2\Delta_\phi)_r}{r!}\right)^{k_r}},$$
 (5.26)

which leads to

$$\langle 0|H_{\text{eff 2}}|0\rangle = 4n!^2 g^2 \sum_{\vec{k}} \frac{1}{n\Delta_{\phi} + \sum_r rk_r} \prod_r \frac{1}{k_r!} \left(\frac{(2\Delta_{\phi})_r}{r!}\right)^{k_r}$$

$$= 4n! g^2 \sum_{N=0}^{\infty} \frac{a_{2N}}{n\Delta_{\phi} + 2N},$$
(5.27)

where we define the sequence $(a_N)_{N\in\mathbb{N}}$ such that

 $^{^{12}}$ A defect induces the following symmetry breaking $SO(d+1,1) \to SO(p+1,1) \times SO(d-p)$, i.e. the conformal subgroup along the defect is preserved, and rotational symmetry "around" the defect is likewise preserved. Non-zero VEVs of operators are associated to the existence of a natural length-scale: their distance to the defect. Another point of view is that the one-point function of an operator in a DCFT is the two-point function of that same operator with the defect.

 $^{^{13}}$ There is an additional minus sign for LORALY in front of g^2 since the interaction matrix is anti-Hermitian, this does not affect the physical arguments of this section however so we ignore this detail.

$$\forall N \in \mathbb{N}, \quad a_N := n! \sum_{\substack{\sum k_r r = 2N \\ \sum k_r = n}} \prod_r \frac{1}{k_r!} \left(\frac{(2\Delta_\phi)_r}{r!} \right)^{k_r}, \tag{5.28}$$

where we've kept the condition $\Delta_{\vec{k}} > \Delta_T$ implicit. Incidentally, since we merely want to study asymptotics, we drop this condition since including light states in the sum does not affect convergence. While this expression seems intricate, its generating function is fairly simple. For |x| < 1, we can define

$$f(x) = \frac{1}{|1 - x|^{2\Delta_{\phi}}} = \sum_{l=0}^{\infty} \frac{(2\Delta_{\phi})_l}{l!} x^l,$$
 (5.29)

then the multinomial expansion leads to

$$f(x)^{n} = \frac{1}{|1 - x|^{2n\Delta_{\phi}}} = n! \sum_{\sum_{r} k_{r} = n} \left(\prod_{r} \frac{1}{k_{r}!} \left(\frac{(2\Delta_{\phi})_{r}}{r!} \right)^{k_{r}} \right) x^{\sum_{r} rk_{r}}.$$
 (5.30)

Hence, clearly a_N is the coefficient of x^{2N} in the above expansion. Yet we also have another expansion for f^n using Pochhammer symbols:

$$f(x)^{n} = \sum_{N=0}^{\infty} \frac{(2n\Delta_{\phi})_{N}}{N!} x^{N}.$$
 (5.31)

Thus by identification

$$a_N = \frac{(2n\Delta_\phi)_{2N}}{(2N)!},$$
 (5.32)

and the vacuum energy correction is

$$\langle 0|H_{\text{eff }2}|0\rangle = 4n!g^2 \sum_{N=0}^{\infty} \frac{(2n\Delta_{\phi})_{2N}}{(2N)!(n\Delta_{\phi} + 2N)} = 4n!g^2 \int_0^1 dx \sum_{N=0}^{\infty} \frac{(2n\Delta_{\phi})_{2N}}{(2N)!} x^{n\Delta_{\phi} + 2N - 1}$$

$$= 2n!g^2 \int_0^1 dx x^{n\Delta_{\phi} - 1} \left[(1-x)^{-2n\Delta_{\phi}} + (1+x)^{-2n\Delta_{\phi}} \right].$$
(5.33)

The second term is better behaved close to 1 than the first, while they both exhibit the same behavior close to 0. Let's therefore focus on the former:

$$\langle 0|H_{\text{eff }2}|0\rangle \supset 2n!g^2 \int_0^1 dx x^{n\Delta_{\phi}-1} (1-x)^{-2n\Delta_{\phi}} \propto \Gamma\left(1-2n\Delta_{\phi}\right). \tag{5.34}$$

Thus for all observables in the effective theory to converge we at least need $\Delta = n\Delta_{\phi} < 1/2$, which is the same condition we derived previously. One expects this to generalize to $\Delta < (m-1)/m$ for a convergent m-th order contribution to this matrix element of the effective Hamiltonian, as for the criterion (5.23) derived using the Casimir energy. This statement is at least valid for the third order contribution studied in [51]. However, we shall soon see in section 5.5 that these divergences are non-local, i.e. they depend on the matrix element in question. Hence, near marginality the effective theory has divergences and requires renormalization.

5.4 Renormalization of the effective theory: the general picture

The previous section demonstrates that great care must be taken to define a UV-finite theory for Hamiltonian truncation. A prescription for doing so was outlined in [51, 52]. Instead of starting from the truncated Hamiltonian, start with the full theory, and introduce a local regulator ϵ which cures observables of their UV divergences, by discarding integration regions where local operators get closer to each other than ϵ in expressions of physical observables such as the vacuum energy (5.20). This yields poles in ϵ which are absorbed into a finite number of counter-terms computed to some order N in perturbation theory, the deformation being relevant, so that we arrive at the renormalized Hamiltonian

$$H = H_0 + V + H_{\rm ct}(\epsilon) =: H_0 + V(\epsilon).$$
 (5.35)

Next, truncate the theory (5.35) using a cutoff Δ_T . In principle, one could then extrapolate numerical results to $\Delta_T \to \infty$, followed by $\epsilon \to 0$. However, this double extrapolation seems quite involved, and this is where effective Hamiltonians come in, since they improve results for smaller Δ_T as we previously noticed. Now compute the effective

Hamiltonian (5.14) associated to (5.35) up to N orders to match the order in perturbation theory of the counter-terms. This gives us some $H_{\text{eff}}(\epsilon)$ which is finite as $\epsilon \to 0$. Hence, upon taking the $\epsilon \to 0$ limit, one obtains

$$H_{\text{eff}} := H_0 + V + K = \lim_{\epsilon \to 0} H_{\text{eff}}(\epsilon). \tag{5.36}$$

To wrap up this discussion, we'll specialize this to the case of 1D CFTs, and LORI and LORALY specifically.

5.5 Renormalization of one-dimensional effective theories

Let's specialize the discussion of the previous section to CFT on the 1D cylinder, the general d-dimensional case being presented in [51]. Suppose our deforming operator is ϕ_{Δ} of dimension Δ , such as on the one-dimensional cylinder our potential be $V=g:(\phi_{\Delta,L}(0)+\phi_{\Delta,R}(0)):$ For simplicity, let's write $\phi_{\Delta}(0)=:(\phi_{\Delta,L}(0)+\phi_{\Delta,R}(0)):$ and let's now denote sums over heavy states using \sum_h . The second order correction is therefore

$$\langle f|H_{\text{eff}}^{(2)}|i\rangle = g^2 \sum_{h} \frac{\langle f|\phi_{\Delta}|h\rangle\langle h|\phi_{\Delta}|i\rangle}{\Delta_{fh}} = -g^2 \int_{-\infty}^{0} d\tau \sum_{h} e^{\tau \Delta_{hf}} \langle f|\phi_{\Delta}(0)|h\rangle\langle h|\phi_{\Delta}(0)|i\rangle.$$
 (5.37)

Let's time evolve using the exponential factors acting on the eigenstates and going from the cylinder to the plane yields

$$\langle f|H_{\text{eff}}^{(2)}|i\rangle = -g^2 \int_{-1}^1 dx |x|^{\Delta - 1} \sum_h \langle f|\phi_{\Delta}(x)|h\rangle \langle h|\phi_{\Delta}(1)|i\rangle.$$
 (5.38)

We can temporarily ignore the insertion of a complete set over the heavy states. Radial quantization tells us that there exist some local operators \mathcal{O}_i , \mathcal{O}_f such that $|i\rangle = \mathcal{O}_i(0)|0\rangle$ and $\langle f| = \langle 0|\mathcal{O}(\infty)$ with $\mathcal{O}(\infty) := \lim_{x\to\infty} |x|^{2\Delta_{\mathcal{O}}}\mathcal{O}(x)$. Next, in the |1-x| < 1 region, let's insert a complete set of local operators over the entire spectrum of the theory, and radial quantize relative to 1:

$$-g^{2} \int_{-1}^{1} dx |x|^{\Delta - 1} \langle \mathcal{O}_{f}(\infty) \phi_{\Delta}(x) \phi_{\Delta}(1) \mathcal{O}_{i}(0) \rangle = -g^{2} \sum_{\mathcal{O}} \int_{0}^{1} dx |x|^{\Delta - 1} \langle \mathcal{O}_{f}(\infty) \mathcal{O}(1) \mathcal{O}_{i}(0) \rangle \langle \mathcal{O}(\infty) \phi_{\Delta}(1) \phi_{\Delta}(x) \rangle$$

$$-g^{2} \sum_{\mathcal{O}} \int_{-1}^{0} dx |x|^{\Delta - 1} \langle \mathcal{O}_{f}(\infty) \phi_{\Delta}(1) \phi_{\Delta}(x) \mathcal{O}_{i}(0) \rangle.$$

$$(5.39)$$

The sums in this decomposition involve integrals which behave nicely in the region $x \to 0$. This is due to the fact that this region corresponds to $\tau \to -\infty$ on the half-cylinder in the original expression (5.37), and the integral is convergent there. As for $x \to 1$, there may be a divergence. We therefore introduce a regulator ϵ such that

$$\langle f|H_{\text{eff}}^{(2)}|i\rangle = -g^2 \sum_{\mathcal{O}} \langle f|\mathcal{O}(1)|i\rangle \int_0^{1-\epsilon} dx |x|^{\Delta-1} \langle \mathcal{O}(\infty)\phi_{\Delta}(1)\phi_{\Delta}(x)\rangle$$

$$-g^2 \sum_{\mathcal{O}} \int_{-1}^0 dx |x|^{\Delta-1} \langle f|\phi_{\Delta}(1)\phi_{\Delta}(x)|i\rangle.$$
(5.40)

Lastly, we reintroduce the complete set of heavy states:

$$\langle f|H_{\text{eff}}^{(2)}|i\rangle = -g^2 \sum_{\mathcal{O}} \langle f|\mathcal{O}(1)|i\rangle \int_0^{1-\epsilon} dx |x|^{\Delta-1} \sum_{\Delta_h > \Delta_T - \Delta_i} \langle \mathcal{O}(\infty)\phi_{\Delta}(1)|h\rangle \langle h|\phi_{\Delta}(x)\rangle - g^2 \sum_{\mathcal{O}} \int_{-1}^0 dx |x|^{\Delta-1} \sum_{\Delta_h > \Delta_T} \langle f|\phi_{\Delta}(1)|h\rangle \langle h|\phi_{\Delta}(x)|i\rangle.$$
(5.41)

where in the first term dependence on $|i\rangle$ is conserved, in order to conserve the appropriate scaling behavior of the integrand. The second term is finite, so we no longer worry about it. Let's henceforth assume \mathcal{O} is primary for a simpler derivation ¹⁴. Note that conformal invariance constrains the following three-point function:

$$\langle \mathcal{O}(\infty)\phi_{\Delta}(1)\phi_{\Delta}(x)\rangle = \frac{\lambda_{\mathcal{O}\Delta\Delta}}{|1-x|^{2\Delta-\Delta_{\mathcal{O}}}} = \lambda_{\mathcal{O}\Delta\Delta} \sum_{n=0}^{\infty} \frac{(2\Delta-\Delta_{\mathcal{O}})_n}{n!} x^n, \qquad (5.42)$$

so that

 $^{^{-14}}$ This actually holds true in one dimension, since later on in this derivation \mathcal{O} is required to have dimension less than one, thus excluding all descendants.

$$H_{\text{eff}}^{(2)}(\epsilon)_{fi} = -g^2 \sum_{\mathcal{O}} \langle f|\mathcal{O}(1)|i\rangle \lambda_{\mathcal{O}\Delta\Delta} \int_{-1}^{1-\epsilon} dx \sum_{n>\Delta'_{T,i}}^{\infty} \frac{(2\Delta - \Delta_{\mathcal{O}})_n}{n!} |x|^{\Delta - 1} x^n + O(\epsilon^0), \qquad (5.43)$$

where again the cutoff $\Delta'_{T,i} := \Delta_T - \Delta_i - \Delta$ depends on the initial state. Performing the integral over x leads to 15

$$H_{\text{eff}}^{(2)}(\epsilon)_{fi} = -g^2 \sum_{\mathcal{O}} \langle f|\mathcal{O}(1)|i\rangle \lambda_{\mathcal{O}\Delta\Delta} \sum_{2n > \Delta'_{T,i}} \frac{\left[1 + (1 - \epsilon)^{2n + \Delta}\right](2\Delta - \Delta_{\mathcal{O}})_{2n}}{(2n)!(2n + \Delta)} + O(\epsilon^0). \tag{5.44}$$

Note that this is divergent when $2\Delta - \Delta_{\mathcal{O}} \geq 1$, in which case we get a harmonic divergence in the $\epsilon \to 0$ limit. Now let's renormalize our effective theory, following the three steps prescribed in [51] and recalled in the previous section 5.4. First, one renormalizes the fundamental theory by introducing relevant local counter-terms:

$$H_0 + V \to H_0 + V + \sum_{2\Delta - \Delta_{\mathcal{O}} \ge 1} g^{\mathcal{O}} : (\mathcal{O}_L(0) + \mathcal{O}_R(0)) :$$
 (5.45)

where the couplings $g^{\mathcal{O}}$ are bare, and are related to renormalized and counter-term couplings via $g^{\mathcal{O}} = g_{\text{ren}}^{\mathcal{O}} + g_{\text{ct}}^{\mathcal{O}}(\epsilon)$. The convenient choice for $g_{\text{ct}}^{\mathcal{O}}(\epsilon)$ is to cancel the divergence in the first term of (5.40):

$$g_{\text{ct}}(\epsilon) = g^2 \int_0^{1-\epsilon} dx |x|^{\Delta - 1} \langle \mathcal{O}(\infty) \phi_{\Delta}(1) \phi_{\Delta}(x) \rangle$$

$$= g^2 \lambda_{\mathcal{O}\Delta\Delta} \sum_{n=0}^{\infty} \frac{[1 + (1 - \epsilon)^{2n + \Delta}](2\Delta - \Delta_{\mathcal{O}})_{2n}}{(2n)!(2n + \Delta)}.$$
(5.46)

Next, we work with the renormalized variables, and derive the corresponding effective Hamiltonian, arriving at:

$$(H_{\text{eff }2})_{fi} = \sum_{2\Delta - \Delta_{\mathcal{O}} > 1} g_{\text{ren}}^{\mathcal{O}} \langle f | \mathcal{O}(1) | i \rangle + 2g^2 \sum_{2\Delta - \Delta_{\mathcal{O}} \ge 1} \langle f | \mathcal{O}(1) | i \rangle \lambda_{\mathcal{O}\Delta\Delta} \sum_{0 < 2n < \Delta'_{T_n}} \frac{(2\Delta - \Delta_{\mathcal{O}})_{2n}}{(2n)!(2n + \Delta)} + \dots$$
 (5.47)

where dots indicate finite values in the limit $\Delta_T \to \infty$, while the sum over n is divergent in the same limit. In order to cure our effective Hamiltonian of this divergence, we add a new counter-term. In a Hamiltonian analogue of the minimal subtraction scheme, we choose:

$$K_2 = \sum_{2\Delta - \Delta_{\mathcal{O}} \ge 1} \langle f | \mathcal{O}(1) | i \rangle \left(g_{\text{ren}}^{\mathcal{O}} + 2g^2 \lambda_{\mathcal{O}\Delta\Delta} \sum_{0 \le 2n \le \Delta'_{T,i}} \frac{(2\Delta - \Delta_{\mathcal{O}})_{2n}}{(2n)!(2n + \Delta)} \right) + \dots$$
 (5.48)

At first glance, the sum over operators might seem daunting for numerical purposes. However, very few operators satisfy this, particularly in one dimension. Indeed, we have $\Delta = 1 - \varepsilon$, hence we sum over \mathcal{O} satisfying $1 - 2\varepsilon \ge \Delta_{\mathcal{O}}$. Depending on the value of ε , we can have at most $\mathbb{1}$, ϕ and ϕ^2 involved in K_2 . However, $\lambda_{\phi\phi^3\phi^3} = \lambda_{\phi\phi^4\phi^4} = 0$ in the UV, hence we may safely discard the non-local ϕ interaction, the local one being also unphysical since it is merely a shift in the VEV of ϕ we conventionally set to zero. Let's summarize the allowed operators below.

- LORI. For $\varepsilon < 1/3$, we can have 1 and ϕ^2 . For $1/3 < \varepsilon < 1/2$, we can only have 1.
- LORALY. For $\varepsilon < 1/4$, we can have 1 and ϕ^2 . For $1/4 < \varepsilon < 1/2$, we can only have 1.

Note that we've also discarded non \mathbb{Z}_2 -symmetric terms in LORI, but do no such thing in LORALY which is not a \mathbb{Z}_2 -symmetric theory. Since we'll need the corresponding OPE coefficients, we compute them using simple diagrammatics in the free theory:

$$\langle \phi^2(0)\phi^4(x)\phi^4(y)\rangle_0 = \bigodot^{\phi^2} = \frac{192}{|x|^{2\Delta_{\phi}}|y|^{2\Delta_{\phi}}|x-y|^{6\Delta_{\phi}}}, \tag{5.49}$$

$$\langle \phi^2(0)\phi^3(x)\phi^3(y)\rangle_0 = \bigcirc = \frac{36}{|x|^{2\Delta_{\phi}}|y|^{2\Delta_{\phi}}|x-y|^{6\Delta_{\phi}}}.$$
 (5.50)

¹⁵This bears a striking resemblance to the series expression (5.33). The two computations are morally the same, although studying the divergence of an arbitrary matrix element of the effective Hamiltonian requires fancier tricks.

Hence $\lambda_{\phi^2\phi^4\phi^4} = 192$, $\lambda_{\phi^2\phi^3\phi^3} = 36$, and of course $\lambda_{1\phi^4\phi^4} = 24$, $\lambda_{1\phi^3\phi^3} = 6$ which are nothing but the normalizations of $\langle \phi^4\phi^4 \rangle$ and $\langle \phi^3\phi^3 \rangle$. In summary, going back to the cylinder:

$$K_2^{\text{LORI}} = \delta_{fi} \left(g_0 + \frac{\lambda^2}{12} \sum_{0 \le 2n \le \Delta_T - \Delta_i - 1 + \varepsilon} \frac{(2 - 2\varepsilon)_{2n}}{(2n)!(2n + 1 - \varepsilon)} \right)$$

$$+ \langle f | \phi^2 | i \rangle \left(g_2 + \frac{\lambda^2}{3} \sum_{0 \le 2n \le \Delta_T - \Delta_i - 1 + \varepsilon} \frac{(3 - 3\varepsilon)_{2n}}{(2n)!(2n + 1 - \varepsilon)} \right) + \dots,$$

$$(5.51)$$

$$K_2^{\text{LORALY}} = \delta_{fi} \left(g_0 - \frac{g^2}{3} \sum_{0 \le 2n \le \Delta_T - \Delta_i - 1 + \varepsilon} \frac{(2 - 2\varepsilon)_{2n}}{(2n)!(2n + 1 - \varepsilon)} \right)$$

$$+ \langle f | \phi^2 | i \rangle \left(g_2 - g^2 \sum_{0 \le 2n \le \Delta_T - \Delta_i - 1 + \varepsilon} \frac{(3 - 3\varepsilon)_{2n}}{(2n)!(2n + 1 - \varepsilon)} \right) + \dots$$

$$(5.52)$$

We defer the detailed study of this renormalized effective theory to further work.

6 Conclusion

The long-range Ising and Lee-Yang models viewed as non-local CFTs on the ∂AdS_2 cylinder are useful testing grounds for Hamiltonian truncation. We have shown that finding the corresponding fixed points is a straightforward root-finding exercise related to conformality conditions, provided we tune all relevant couplings of a given theory. More specifically, imposing a vanishing ground-state energy, the expected descendant at $\Delta_{\phi} + 1$ and the equations of motion fixes the counter-terms unambiguously; the resulting spectra match the one or two-loop ε -expansion data to the accuracy of our numerics. This agreement confirms that the truncated theory reaches the correct interacting fixed points despite working with a finite Hilbert space.

A systematic improvement comes from the next-to-leading-order effective Hamiltonian obtained by integrating out states above the cutoff more carefully. Even for modest truncation levels, these corrections significantly improve convergence with the UV cutoff, as in the case of Δ_{ϕ^2} for LORI, hence showing that reliable results do not necessarily require prohibitively large bases. We also noticed contrasts between LORI and LORALY, in that the leading order corrections to LORI were truncation-independent, while those to LORALY were not, leading to slower convergence for LORALY. Since the construction parallels standard Rayleigh–Schrödinger perturbation theory, its extension to higher orders is straightforward. On the perturbative side, pushing the ε -expansion to higher loops will provide sharper benchmarks for both scaling dimensions and OPE coefficients. We've chosen to stop at two loops for uniformity between the available and derived data for LORI, and the data we derived for LORALY, the latter being less studied in the literature. However, in the case of LORI results to three loops have been derived in [68, 69] and comparison with Hamiltonian truncation is straightforward.

Several refinements remain to be addressed. We encountered UV divergences in the effective Hamiltonian at next-to-leading order. We subsequently outlined a procedure for rendering this effective Hamiltonian finite at fixed cutoff Δ_T , and derived the corresponding non-local counter-terms. A detailed numerical treatment of the UV divergences should be implemented to test the renormalized effective Hamiltonian thus derived. In addition, computing three-point matrix elements within the present setup would supply the full operator data $\{\Delta_i, \lambda_{ijk}\}$, enabling a direct, quantitative comparison with numerical bootstrap bounds. Ultimately, our aim is to understand how bootstrap methods relate to Hamiltonian truncation methods, and reproduce the spectra of solutions to crossing relations. This will be the subject of further study.

A Useful integrals

A.1 GFF propagator

As a prerequisite to using Wick's theorem for calculating correlators, we need to calculate a fundamental building block: the propagator of the GFF theory. It is given by the Green's function of the fractional Laplacian, which can be solved for using the Fourier transform:

$$G(x_1 - x_2) = \int \frac{d^d p}{(2\pi)^d} \frac{e^{ip \cdot (x_1 - x_2)}}{|p|^{\sigma}}.$$
 (A.1)

If it is consistent with CFT, this quantity must go like $|x-y|^{-2\Delta_{\phi}}$. To show that this holds, we use the following identity (easily derived using a change of variables in the definition of the Γ -function):

$$\frac{1}{|p|^{\sigma}} = \frac{1}{\Gamma\left(\frac{\sigma}{2}\right)} \int_0^{+\infty} t^{\frac{\sigma}{2} - 1} e^{-t|p|^2} dt. \tag{A.2}$$

Next, we plug this into equation (A.1). This implies (integrals can be swapped using Fubini's theorem):

$$G(x) = \frac{1}{\Gamma\left(\frac{\sigma}{2}\right)} \int_0^{+\infty} dt t^{\frac{\sigma}{2} - 1} \int \frac{d^d p}{(2\pi)^d} e^{-t|p|^2 + ipx}. \tag{A.3}$$

The momentum space integral is a well-known Gaussian integral, whose evaluation yields:

$$G(x) = \frac{1}{(4\pi)^{\frac{d}{2}} \Gamma(\frac{\sigma}{2})} \int_0^{+\infty} dt e^{-\frac{|x|^2}{4t}} t^{\frac{\sigma - d}{2} - 1}.$$
 (A.4)

Next, the change of variables $u = |x|^2/(4t)$ turns the remaining integral into a Γ -function, and we obtain the desired result:

$$G(x) = \frac{2^{d-\sigma} \Gamma\left(\frac{d-\sigma}{2}\right)}{(4\pi)^{\frac{d}{2}} \Gamma\left(\frac{\sigma}{2}\right)} \frac{1}{|x|^{d-\sigma}} = \frac{\mathcal{N}_{\sigma}}{|x|^{2\Delta_{\phi}}}.$$
 (A.5)

We can then use the normalization factor in front of the GFF action to tune the propagator to the conventional form $G(x-y) = |x-y|^{-2\Delta_{\phi}}$. This leads to a slightly unusual normalization in momentum space:

$$G(p) = \frac{1}{\mathcal{N}_{\sigma}|p|^{\sigma}}.$$
 (A.6)

A.2 Convolution formula

Nearly every Feynman diagram we compute in this work makes use of the following "convolution" identity:

$$I(x) := \int \frac{d^d y}{|x - y|^A |y|^B} = \frac{w_A w_B}{w_{A+B-d}} \frac{1}{|x|^{A+B-d}}.$$
 (A.7)

where $w_A = (4\pi)^{d/2} 2^{-A} \Gamma\left(\frac{d-A}{2}\right) / \Gamma\left(\frac{A}{2}\right)$. Since it is a key ingredient in previous computations and it is easily derived using the Gaussian theory's propagator, we provide a derivation in this section. The main idea is to calculate it in momentum space, and then perform an inverse Fourier transform back to position space. The Fourier transform of I obeys

$$I(p) := \int \frac{d^d x d^d y e^{-ipx}}{|x - y|^A |y|^B} = \int \frac{d^d x d^d y e^{-ip(x+y)}}{|x|^A |y|^B} = (2\pi)^{2d} G_A(p) G_B(p),$$
(A.8)

where we've applied a translation by +y to x (this is of course a general result regarding Fourier transforms of convolutions), and $G_A(p) := \mathcal{N}_A |p|^{A-d}$ (leveraging our knowledge of the propagator). Transforming back to position space yields

$$I(x) = (2\pi)^{2d} \mathcal{N}_A \mathcal{N}_B \int \frac{d^d p}{(2\pi)^d} \frac{e^{ipx}}{|p|^{2d-A-B}} = (2\pi)^{2d} \mathcal{N}_A \mathcal{N}_B \mathcal{N}_{2d-A-B} \frac{1}{|x|^{A+B-d}}$$
(A.9)

Using the values of the \mathcal{N}_A coefficients derived in section A.1 leads to the desired result.

A.3 Extraction of divergences

Let's review another elementary, although very useful result in QFT. In this work, we often had to deal with intricate Feynman diagrams, whose full closed-form expression was not essential to the derivation of fixed points and physical observables. Suppose we're given a diagram which blows up in the ε -expansion as $\varepsilon \to 0$. This typically happens as internal vertices get close to each other and to external insertions. In this limit, one usually ends up with an integral of the form

$$I_{\varepsilon} = \int \frac{d^d y}{|y|^{d - K\varepsilon}} \tag{A.10}$$

for some constant K > 0. To extract the divergence of this logarithmically divergent quantity, we isolate the problematic $y \to 0$ region, and introduce a UV regulator Λ :

$$I_{\varepsilon} \supset \int_{\Lambda}^{1} \frac{d^{d}y}{|y|^{d-K\varepsilon}} = \frac{2\pi^{\frac{d}{2}}}{\Gamma\left(\frac{d}{2}\right)K\varepsilon} \left(1 - \Lambda^{K\varepsilon}\right) , \tag{A.11}$$

and for fixed ε , we take the limit $\Lambda \to 0$. This yields

$$I_{\varepsilon} \supset \frac{2\pi^{\frac{d}{2}}}{\Gamma\left(\frac{d}{2}\right)K\varepsilon},$$
 (A.12)

which is our desired pole as $\varepsilon \to 0$.

B Diagrammatics

B.1 Hard diagram in the renormalization of ϕ^2

The diagram

is difficult to compute exactly. Let's therefore extract its divergence, which is enough in the MS scheme. There are three relevant regions: $y, z \to 0$, $y, z \to x$ and $y \sim z$. Since the setup is symmetric in 0 and x, we can study $y, z \to 0$ and account for $y, z \to x$ by multiplying by 2:

$$\frac{1}{|x|^{4\Delta_{\phi}}}\int\frac{d^dyd^dz}{|y|^{2\Delta_{\phi}}|z|^{2\Delta_{\phi}}|y-z|^{4\Delta_{\phi}}} = \frac{1}{|x|^{4\Delta_{\phi}}}\frac{w_{4\Delta_{\phi}}w_{2\Delta_{\phi}}}{w_{6\Delta_{\phi}-d}}\int\frac{d^dy}{|y|^{8\Delta_{\phi}-d}} = -\frac{\pi^{\frac{d}{2}}}{\Gamma\left(\frac{d}{2}\right)\varepsilon}\frac{w_{4\Delta_{\phi}}w_{2\Delta_{\phi}}}{w_{6\Delta_{\phi}-d}}\frac{1}{|x|^{4\Delta_{\phi}}}\,. \tag{B.2}$$

As for $y \sim z$:

$$\int \frac{d^d y d^d z}{|y|^{2\Delta_{\phi}} |z|^{2\Delta_{\phi}} |y - z|^{4\Delta_{\phi}} |x - y|^{4\Delta_{\phi}}} = \frac{w_{2\Delta_{\phi}} w_{4\Delta_{\phi}}}{w_{6\Delta_{\phi} - d}} \int \frac{d^d y}{|y|^{8\Delta_{\phi} - d} |x - y|^{4\Delta_{\phi}}} = \frac{w_{2\Delta_{\phi}} w_{4\Delta_{\phi}}^2 w_{8\Delta_{\phi} - d}}{w_{6\Delta_{\phi} - d} w_{12\Delta_{\phi} - 2d}} \frac{1}{|x|^{12\Delta_{\phi} - 2d}}.$$
(B.3)

Hence

$$\phi^2 \left(\bigcap \right) \phi^2 \supset 2\lambda^2 \mu^{2\varepsilon} \left(-\frac{2\pi^{\frac{d}{2}}}{\Gamma\left(\frac{d}{2}\right)\varepsilon} \frac{w_{4\Delta_{\phi}} w_{2\Delta_{\phi}}}{w_{6\Delta_{\phi}-d}} \frac{1}{|x|^{4\Delta_{\phi}}} + \frac{w_{2\Delta_{\phi}} w_{4\Delta_{\phi}}^2 w_{8\Delta_{\phi}-d}}{w_{6\Delta_{\phi}-d} w_{12\Delta_{\phi}-2d}} \frac{1}{|x|^{12\Delta_{\phi}-2d}} \right), \tag{B.4}$$

B.2 Anomalous dimension of ϕ^4 to one-loop order

To maintain consistency with the data derived for LORI in section 3.2 and justify the result in section 3.3.3, let's also derive the anomalous dimension of ϕ^4 . Generally, computing anomalous dimensions for LORALY is more challenging, since we need to get to higher order in the coupling than in LORI for a given order in ε . Hence, let's stop at one loop for ϕ^4 in LORALY. Let's look at $\langle \phi^4(0)\phi^4(x)\rangle$. At tree level:

$$\phi^4 \qquad \qquad \phi^4 = \frac{24}{|x|^{8\Delta_{\phi}}} \,. \tag{B.5}$$

At one loop, the relevant diagrams are:

$$\phi^4 \qquad \qquad \phi^4 = -144g^2 \left(\frac{w_{4\Delta_{\phi}} w_{2\Delta_{\phi}}}{w_{6\Delta_{\phi} - d}}\right)^2 \frac{1}{|x|^{14\Delta_{\phi} - 2d}}, \tag{B.6}$$

$$\phi^4 \qquad \qquad \phi^4 = -72g^2 \frac{w_{2\Delta_{\phi}} w_{4\Delta_{\phi}}^2}{w_{10\Delta_{\phi} - 2d}} \frac{1}{|x|^{14\Delta_{\phi} - 2d}}, \tag{B.7}$$

$$\phi^4 \qquad \qquad \phi^4 = -72g^2 \frac{w_{4\Delta_{\phi}} w_{2\Delta_{\phi}}^2}{w_{8\Delta_{\phi} - 2d}} \frac{1}{|x|^{14\Delta_{\phi} - 2d}}, \tag{B.8}$$

$$\phi^{4} \qquad \phi^{4} = -\frac{288g^{2}\pi^{\frac{d}{2}}w_{2\Delta_{\phi}}^{2}}{\Gamma\left(\frac{d}{2}\right)w_{4\Delta_{\phi}-d}}\frac{1}{\varepsilon}\frac{1}{|x|^{8\Delta_{\phi}}}, \qquad (B.9)$$

where it turns out that only the last diagram – the most difficult to compute exactly – is divergent. The corresponding divergence is computed by examining the integral in the region where the interaction vertices simultaneously get close to one of the external insertions, and using the result from appendix A.3. The corresponding renormalization factor is then

$$Z_{\phi^4} = 1 - \frac{6\pi^d \Gamma\left(\frac{d}{6}\right)^3}{\Gamma\left(\frac{d}{3}\right)^3 \Gamma\left(\frac{d}{2}\right)} \frac{g^2}{\varepsilon} + O(g^3).$$
(B.10)

C Anomalous dimensions from β -functions

Let's prove that for an interaction going like $g\mathcal{O}$ in d dimensions, we have:

$$\Delta_{\mathcal{O}} = d + \frac{\partial \beta}{\partial g} \,. \tag{C.1}$$

To prove this, we adapt arguments from [70]. We first assume our theory has a stress tensor, and show that $T^{\mu}_{\mu} = \beta_g \mathcal{O}$. Consider an infinitesimal scale transformation $x \mapsto (1 + \varepsilon)x$. In QFT, this also affects the coupling g. Since energy goes like inverse length, we have:

$$g(\mu) \mapsto g\left(\frac{\mu}{1+\varepsilon}\right) = g(\mu) - \varepsilon\beta_g$$
 (C.2)

We then require that the action remain unchanged during such a transformation:

$$\delta S = \varepsilon \int d^d x \left[\partial_\mu j^\mu - \frac{\partial \mathcal{L}}{\partial g} \beta_g \right] \tag{C.3}$$

where the first term is the classical variation of the action, expressed using the dilatation current $j^{\mu} = T^{\mu}_{\ \nu} x^{\nu}$, $T^{\mu\nu}$ being the stress tensor, and the second is the quantum variation. We've assumed that $\partial \mathcal{L}/\partial g = \mathcal{O}$, hence:

$$\partial_{\mu}j^{\mu} - \frac{\partial \mathcal{L}}{\partial g}\beta_{g} = (\partial_{\mu}T^{\mu}_{\ \nu})x^{\nu} + T^{\mu}_{\ \mu} - \beta_{g}\mathcal{O} = T^{\mu}_{\ \mu} - \beta_{g}\mathcal{O} = 0. \tag{C.4}$$

Next, since one can write $d\mathcal{O}/d\log\mu = -\Delta_O\mathcal{O}$ for any operator \mathcal{O} and using that $\Delta_{T_{\mu\nu}} = d$ is protected, we get on the one hand:

$$\frac{d}{d\log\mu}T^{\mu}_{\ \mu} = -dT^{\mu}_{\ \mu} = -d\beta_g\mathcal{O} \tag{C.5}$$

and on the other:

$$\frac{d}{d\log\mu}T^{\mu}_{\ \mu} = \frac{\partial\beta_g}{\partial g}\beta_g\mathcal{O} - \beta_g\Delta_{\mathcal{O}}\mathcal{O} \tag{C.6}$$

The RHS of the last two equalities being equal to one another leads to the desired result. A final loose end regarding our use of this result for long-range theories is the absence of a stress tensor. However, one might overcome this difficulty by invoking the so-called Caffarelli-Silvestre trick [56, 71]. This amounts to viewing the GFF theory in d dimensions as the dimensional reduction of a massless local free theory in $\bar{d} = d + 2 - \sigma$ fractional dimensions. This strange fractional dimension can be motivated by the fact that $\Delta_{\phi} = (\bar{d} - 2)/2$ is the scaling dimension of a local free field in \bar{d} dimensions. The bulk \bar{d} -dimensional theory then describes a local scalar field $\Phi(z, x)$, where $z \in \mathbb{R}^{\bar{d}-d}$, and $\phi(x) = \Phi(0, x)$. Interations are subsequently added at z = 0 in a similar fashion to the AdS construction in section 2.2. The fractional-dimensional bulk theory is hence a bona fide local theory with a stress tensor, and the relation (C.1) therefore holds true in the full bulk space. It therefore also holds for the long-range theory at z = 0.

References

- 1. Poland, D., Rychkov, S. & Vichi, A. The conformal bootstrap: Theory, numerical techniques, and applications. *Rev. Mod. Phys.* **91**, 015002. https://link.aps.org/doi/10.1103/RevModPhys.91.015002 (1 Jan. 2019).
- 2. Maldacena, J. The large-N limit of superconformal field theories and supergravity. *International journal of theoretical physics* **38**, 1113–1133 (1999).
- 3. Levine, N. & Paulos, M. F. Bootstrapping bulk locality. Part I: Sum rules for AdS form factors 2023. arXiv: 2305.07078 [hep-th]. https://arxiv.org/abs/2305.07078.
- 4. Levine, N. & Paulos, M. F. Bootstrapping bulk locality. Part II: Interacting functionals 2025. arXiv: 2408.00572 [hep-th]. https://arxiv.org/abs/2408.00572.
- 5. Ribault, S. Exactly solvable conformal field theories 2025. arXiv: 2411.17262 [hep-th]. https://arxiv.org/abs/2411.17262.
- 6. Rychkov, S. & Su, N. New Developments in the Numerical Conformal Bootstrap 2024. arXiv: 2311.15844 [hep-th]. https://arxiv.org/abs/2311.15844.
- 7. El-Showk, S. et al. Solving the 3D Ising model with the conformal bootstrap. Physical Review D 86. ISSN: 1550-2368. http://dx.doi.org/10.1103/PhysRevD.86.025022 (July 2012).
- 8. Mazáč, D. & Paulos, M. F. The analytic functional bootstrap. Part I: 1D CFTs and 2D S-matrices. *Journal of High Energy Physics* **2019**. ISSN: 1029-8479. http://dx.doi.org/10.1007/JHEP02(2019)162 (Feb. 2019).
- 9. Mazáč, D., Rastelli, L. & Zhou, X. An analytic approach to BCFTd. *Journal of High Energy Physics* **2019**, 1–63 (2019).
- 10. Ghosh, K., Kaviraj, A. & Paulos, M. F. Polyakov blocks for the 1D conformal field theory mixed-correlator bootstrap. *Physical Review D* **109.** ISSN: 2470-0029. http://dx.doi.org/10.1103/PhysRevD.109.L061703 (Mar. 2024).
- 11. Ghosh, K., Paulos, M. F. & Suchel, N. Solving 1D crossing and QFT₂/CFT₁ 2025. arXiv: 2503.22798 [hep-th]. https://arxiv.org/abs/2503.22798.
- 12. Kennedy, T. & Rychkov, S. Tensor RG approach to high-temperature fixed point. *Journal of Statistical Physics* **187**, 33 (2022).
- 13. Kennedy, T. & Rychkov, S. Tensor Renormalization Group at Low Temperatures: Discontinuity Fixed Point. Annales Henri Poincaré 25, 773-841. ISSN: 1424-0661. http://dx.doi.org/10.1007/s00023-023-01289-y (May 2023).
- 14. Ebel, N., Kennedy, T. & Rychkov, S. Transfer Matrix and Lattice Dilatation Operator for High-Quality Fixed Points in Tensor Network Renormalization Group 2024. arXiv: 2409.13012 [cond-mat.stat-mech]. https://arxiv.org/abs/2409.13012.
- 15. Ebel, N., Kennedy, T. & Rychkov, S. Rotations, Negative Eigenvalues, and Newton Method in Tensor Network Renormalization Group 2025. arXiv: 2408.10312 [cond-mat.stat-mech]. https://arxiv.org/abs/2408.10312.
- 16. Läuchli, A. M., Herviou, L., Wilhelm, P. H. & Rychkov, S. Exact Diagonalization, Matrix Product States and Conformal Perturbation Theory Study of a 3D Ising Fuzzy Sphere Model 2025. arXiv: 2504.00842 [cond-mat.stat-mech]. https://arxiv.org/abs/2504.00842.
- 17. Tiwana, K., Lauria, E. & Tilloy, A. A relativistic continuous matrix product state study of field theories with defects 2025. arXiv: 2501.09797 [hep-th]. https://arxiv.org/abs/2501.09797.
- 18. Tilloy, A. A study of the quantum Sinh-Gordon model with relativistic continuous matrix product states 2022. arXiv: 2209.05341 [hep-th]. https://arxiv.org/abs/2209.05341.
- 19. Delcamp, C. & Tilloy, A. Computing the renormalization group flow of two-dimensional ϕ 4 theory with tensor networks. *Physical Review Research* 2, 033278 (2020).
- 20. Tilloy, A. & Cirac, J. I. Continuous Tensor Network States for Quantum Fields. *Physical Review X* **9.** ISSN: 2160-3308. http://dx.doi.org/10.1103/PhysRevX.9.021040 (May 2019).
- 21. Tilloy, A. Variational method in relativistic quantum field theory without cutoff. *Physical Review D* **104.** ISSN: 2470-0029. http://dx.doi.org/10.1103/PhysRevD.104.L091904 (Nov. 2021).
- 22. Gattringer, C. & Lang, C. Quantum chromodynamics on the lattice: an introductory presentation (Springer Science & Business Media, 2009).
- 23. Schollwöck, U. The density-matrix renormalization group. Reviews of modern physics 77, 259–315 (2005).

- 24. Verstraete, F. et al. Density matrix renormalization group, 30 years on. Nature Reviews Physics 5, 273–276 (2023).
- 25. Brooks III, E. & Frautschi, S. C. Scalars coupled to fermions in 1+ 1 dimensions. Zeitschrift für Physik C Particles and Fields 23, 263–273 (1984).
- 26. Yurov, V. & Zamolodchikov, A. B. Truncated comformal space approach to scaling Lee-Yang model. *International Journal of Modern Physics A* 5, 3221–3245 (1990).
- 27. Yurov, V. & Zamolodchikov, A. B. Truncated-fermionic-space approach to the critical 2D Ising model with magnetic field. *International Journal of Modern Physics A* **6**, 4557–4578 (1991).
- 28. James, A. J., Konik, R. M., Lecheminant, P., Robinson, N. J. & Tsvelik, A. M. Non-perturbative methodologies for low-dimensional strongly-correlated systems: From non-abelian bosonization to truncated spectrum methods. *Reports on Progress in Physics* 81, 046002 (2018).
- 29. Hogervorst, M., Rychkov, S. & van Rees, B. C. Truncated conformal space approach in d dimensions: A cheap alternative to lattice field theory? *Physical Review D* **91**, 025005 (2015).
- 30. Rychkov, S. & Vitale, L. G. Hamiltonian truncation study of the φ^4 theory in two dimensions. *Physical Review* D **91**, 085011 (2015).
- 31. Rychkov, S. & Vitale, L. G. Hamiltonian Truncation Study of the ϕ^4 Theory in Two Dimensions. II. The Z_2 -Broken Phase and the Chang Duality. *Phys. Rev. D* **93**, 065014. arXiv: 1512.00493 [hep-th] (2016).
- 32. Katz, E., Tavares, G. M. & Xu, Y. A solution of 2D QCD at Finite N using a conformal basis 2014. arXiv: 1405.6727 [hep-th]. https://arxiv.org/abs/1405.6727.
- 33. Elias-Miro, J., Montull, M. & Riembau, M. The Renormalized Hamiltonian Truncation Method in the Large E_T Expansion. JHEP 04, 144. arXiv: 1512.05746 [hep-th] (2016).
- 34. Bajnok, Z. & Lajer, M. Truncated Hilbert Space Approach to the 2d ϕ^4 Theory. *JHEP* **10**, 050. arXiv: 1512. 06901 [hep-th] (2016).
- 35. Katz, E., Khandker, Z. U. & Walters, M. T. A Conformal Truncation Framework for Infinite-Volume Dynamics. JHEP 07, 140. arXiv: 1604.01766 [hep-th] (2016).
- 36. Anand, N., Genest, V. X., Katz, E., Khandker, Z. U. & Walters, M. T. RG Flow from ϕ^4 Theory to the 2D Ising Model. *JHEP* **08**, 056. arXiv: 1704.04500 [hep-th] (2017).
- 37. Elias-Miro, J., Rychkov, S. & Vitale, L. G. High-Precision Calculations in Strongly Coupled Quantum Field Theory with Next-to-Leading-Order Renormalized Hamiltonian Truncation. *JHEP* 10, 213. arXiv: 1706.06121 [hep-th] (2017).
- 38. Elias-Miro, J., Rychkov, S. & Vitale, L. G. NLO Renormalization in the Hamiltonian Truncation. *Phys. Rev.* D **96**, 065024. arXiv: 1706.09929 [hep-th] (2017).
- 39. Rutter, D. & van Rees, B. C. Counterterms in Truncated Conformal Perturbation Theory. *JHEP* 07, 052. arXiv: 1803.05798 [hep-th] (2023).
- 40. Fitzpatrick, A. L., Kaplan, J., Katz, E., Vitale, L. G. & Walters, M. T. Lightcone Effective Hamiltonians and RG Flows. *JHEP* 08, 120. arXiv: 1803.10793 [hep-th] (2018).
- 41. Hogervorst, M. RG Flows on S^d and Hamiltonian Truncation. *JHEP* **04**, 048. arXiv: 1811.00528 [hep-th] (2019).
- 42. Delacrétaz, L. V., Fitzpatrick, A. L., Katz, E. & Vitale, L. G. Conformal Truncation of Chern-Simons Theory at Large N_f . JHEP 03, 107. arXiv: 1811.10612 [hep-th] (2019).
- 43. Anand, N., Khandker, Z. U. & Walters, M. T. Momentum Space CFT Correlators for Hamiltonian Truncation. JHEP 10, 095. arXiv: 1911.02573 [hep-th] (2020).
- 44. Fitzpatrick, A. L., Katz, E., Walters, M. T. & Xin, Y. Solving the 2D SUSY Gross-Neveu-Yukawa Model with Conformal Truncation. *JHEP* **01**, 182. arXiv: 1911.10220 [hep-th] (2021).
- 45. Elias-Miro, J. & Hardy, E. Exploring Hamiltonian Truncation in d = 2 + 1. Phys. Rev. D 102, 065001. arXiv: 2003.08405 [hep-th] (2020).
- 46. Anand, N. et al. Introduction to Lightcone Conformal Truncation: QFT Dynamics from CFT Data. arXiv preprint. arXiv: 2005.13544 [hep-th] (2020).
- 47. Anand, N., Katz, E., Khandker, Z. U. & Walters, M. T. Nonperturbative Dynamics of (2+1)d ϕ^4 -Theory from Hamiltonian Truncation. *JHEP* **05**, 190. arXiv: 2010.09730 [hep-th] (2021).
- 48. Hogervorst, M., Meineri, M., Penedones, J. & Salehi Vaziri, K. Hamiltonian Truncation in Anti-de Sitter Spacetime. *JHEP* **08**, 063. arXiv: 2104.10689 [hep-th] (2021).

- 49. Francesco, P., Mathieu, P. & Sénéchal, D. Conformal field theory (Springer Science & Business Media, 2012).
- 50. Cohen, T., Farnsworth, K., Houtz, R. & Luty, M. Hamiltonian truncation effective theory. *SciPost Physics* 13, 011 (2022).
- 51. Miró, J. E. & Ingoldby, J. Effective Hamiltonians and counterterms for Hamiltonian truncation. *Journal of High Energy Physics* **2023**, 1–35 (2023).
- 52. Delouche, O., Elias Miro, J. & Ingoldby, J. Hamiltonian truncation crafted for UV-divergent QFTs. *SciPost Physics* **16**, 105 (2024).
- 53. Cardy, J. The Yang-Lee Edge Singularity and Related Problems 2023. arXiv: 2305.13288 [cond-mat.stat-mech]. https://arxiv.org/abs/2305.13288.
- 54. Yang, C.-N. & Lee, T.-D. Statistical theory of equations of state and phase transitions. I. Theory of condensation. *Physical Review* 87, 404 (1952).
- 55. Lee, T.-D. & Yang, C.-N. Statistical theory of equations of state and phase transitions. II. Lattice gas and Ising model. *Physical Review* 87, 410 (1952).
- 56. Paulos, M. F., Rychkov, S., van Rees, B. C. & Zan, B. Conformal invariance in the long-range Ising model. Nuclear Physics B 902, 246-291. ISSN: 0550-3213. https://www.sciencedirect.com/science/article/pii/S0550321315003703 (2016).
- 57. Witten, E. Anti De Sitter Space And Holography 1998. arXiv: hep-th/9802150.
- 58. Bianchi, L., Cardinale, L. S. & de Sabbata, E. Defects in the long-range O(N) model 2024. arXiv: 2412.08697 [hep-th]. https://arxiv.org/abs/2412.08697.
- 59. Kleinert, H. & Schulte-Frohlinde, V. Critical Properties of ϕ^4 -theories (World Scientific, 2001).
- 60. Giombi, S. & Khanchandani, H. O(N) models with boundary interactions and their long range generalizations. Journal of High Energy Physics 2020, 1–53 (2020).
- 61. Behan, C., Lauria, E., Nocchi, M. & van Vliet, P. Analytic and numerical bootstrap for the long-range Ising model. *Journal of High Energy Physics* **2024**, 1–62 (2024).
- 62. Behan, C., Rastelli, L., Rychkov, S. & Zan, B. A scaling theory for the long-range to short-range crossover and an infrared duality*. *Journal of Physics A: Mathematical and Theoretical* **50**, 354002. https://dx.doi.org/10.1088/1751-8121/aa8099 (Aug. 2017).
- 63. Behan, C. C. Bootstrapping some continuous families of conformal field theories PhD thesis (Stony Brook U., 2019).
- 64. Macfarlane, A. & Woo, G. φ^3 theory in six dimensions and the renormalization group. Nuclear Physics B 77, 91–108 (1974).
- 65. Sterman, G. An Introduction to quantum field theory (Cambridge university press, 1993).
- 66. Grinstein, B., Stergiou, A., Stone, D. & Zhong, M. Two-loop renormalization of multiflavor ϕ^3 theory in six dimensions and the trace anomaly. *Physical Review D* **92**, 045013 (2015).
- 67. Penedones, J. TASI Lectures on AdS/CFT in New Frontiers in Fields and Strings (WORLD SCIENTIFIC, Nov. 2016). http://dx.doi.org/10.1142/9789813149441_0002.
- 68. Benedetti, D., Gurau, R., Harribey, S. & Suzuki, K. Long-range multi-scalar models at three loops. *Journal of Physics A: Mathematical and Theoretical* **53**, 445008. ISSN: 1751-8121. http://dx.doi.org/10.1088/1751-8121/abb6ae (Oct. 2020).
- 69. Benedetti, D., Gurau, R. & Harribey, S. Addendum: Long-range multi-scalar models at three loops (2020 J. Phys. A: Math. Theor. 53 445008). *Journal of Physics A: Mathematical and Theoretical* 58, 129401. ISSN: 1751-8121. http://dx.doi.org/10.1088/1751-8121/adbfe4 (Mar. 2025).
- 70. Gubser, S. S., Nellore, A., Pufu, S. S. & Rocha, F. D. Thermodynamics and Bulk Viscosity of Approximate Black Hole Duals to Finite Temperature Quantum Chromodynamics. *Phys. Rev. Lett.* **101**, 131601. https://link.aps.org/doi/10.1103/PhysRevLett.101.131601 (13 Sept. 2008).
- 71. Caffarelli, L. & Silvestre, L. An Extension Problem Related to the Fractional Laplacian. Communications in Partial Differential Equations 32, 1245–1260. ISSN: 1532-4133. http://dx.doi.org/10.1080/03605300600987306 (Aug. 2007).